คอมพอสิตของเศษยางรถยนต์-อนุภาคแม่เหล็กระดับนาโนเมตรเพื่อเป็นตัวดูดซับสำหรับการขจัดน้ำมันจากน้ำ

นายพีรพัฒน์ นิวาศานนท์

วิทยานิพนธ์นี้เป็นส่วนหนึ่งของการศึกษาตามหลักสูตรปริญญาวิทยาศาสตรมหาบัณฑิต
สาขาวิชาปิโตรเคมีและวิทยาศาสตร์พอลิเมอร์
คณะวิทยาศาสตร์ จุฬาลงกรณ์มหาวิทยาลัย
ปีการศึกษา 2555
ลิขสิทธิ์ของจุฬาลงกรณ์มหาวิทยาลัย

WASTE TYRE RUBBER-MAGNETIC NANOPARTICLE COMPOSITES AS SORBENTS FOR OIL REMOVAL FROM WATER

Mr. Pheeraphat Niwasanon

A Thesis Submitted in Partial Fulfillment of the Requirements

for the Degree of Master of Science Program in Petrochemistry and Polymer Science

Faculty of Science

Chulalongkorn University

Academic Year 2012

Thesis Title	WASTE TYRE RUBBER-MAGNETIC NANOPARTICLE COMPOSITES AS SORBENTS FOR OIL REMOVAL FROM WATER
By	Mr. Pheeraphat Niwasanon
Field of Study	Petrochemistry and Polymer Science
Thesis Advisor	Assistant Professor Apichat Imyim, Ph.D.
Thesis Co-advisor	Numpon Insin, Ph.D.

Accepted by the Faculty of Science, Chulalongkorn University in Partial Fulfillment of the Requirements for the Master's Degree

……. Dean of the Faculty of Science
(Professor Supot Hannongbua, Dr. rer. nat.)

THESIS COMMITTEE

…….. Chairman
(Assistant Professor Warinthorn Chavasiri, Ph.D.)

……. Thesis Advisor
(Assistant Professor Apichat Imyim, Ph.D.)

…….. Thesis Co-advisor
(Numpon Insin, Ph.D.)

…….. Examiner
(Amarawan Intasiri, Ph.D.)

…….. External Examiner
(Assistant Professor Anawat Pinisakul, Ph.D.)

พีรพัฒน์ นิวาศานนท์ : คอมพอสิตของเศษยางรถยนต์-อนุภาคแม่เหล็กระดับนาโนเมตรเพื่อเป็นตัวดูดซับสำหรับการขจัดน้ำมันจากน้ำ. (WASTE TYRE RUBBER-MAGNETIC NANOPARTICLE COMPOSITES AS SORBENTS FOR OIL REMOVAL FROM WATER) อ. ที่ปรึกษาวิทยานิพนธ์หลัก : ผศ. ดร.อภิชาติ อิ่มยิ้ม, อ. ที่ปรึกษาวิทยานิพนธ์ร่วม : ดร.นำพล อินสิน, 79 หน้า.

ปริมาณขยะจากยางรถยนต์ที่ใช้แล้วมีปริมาณเพิ่มสูงขึ้น และยังไม่มีวิธีกำจัดที่เหมาะสม เนื่องจากขยะจากยางรถยนต์ย่อยสลายยาก นอกจากนี้ ปัญหาของน้ำมันที่มีการปนเปื้อนลงสู่แหล่งน้ำยังเป็นปัญหาสิ่งแวดล้อมอีกปัญหาหนึ่งที่ต้องได้รับการแก้ไข งานวิจัยนี้จึงนำยางรถยนต์มาใช้เป็นตัวดูดซับสำหรับกำจัดน้ำมันออกจากผิวน้ำ โดยการสังเคราะห์คอมพอสิตระหว่างยางรถยนต์กับอนุภาคแม่เหล็กระดับนาโนเมตร เพื่อให้สามารถใช้แรงแม่เหล็กช่วยให้ง่ายในการจัดเก็บตัวดูดซับออกจากแหล่งน้ำ โดยใช้อนุภาคแม่เหล็กเป็นเหล็กออกไซด์ที่สังเคราะห์จากสารเชิงซ้อนเหล็กโอลิเอต ด้วยวิธี Thermal decomposition ซึ่งเป็นวิธีที่สามารถควบคุมขนาดอนุภาคแม่เหล็กให้ใกล้เคียงกัน และสังเคราะห์คอมพอสิตด้วยการดูดซับอนุภาคแม่เหล็กโดยยางรถยนต์ในตัวทำละลายชนิดต่าง ๆ ได้แก่ เฮกเซน, เอทิลแอซีเทต, โทลูอีน, คลอโรฟอร์ม, เบนซีน และอะซิโตน โดยทำการศึกษาเวลาและความเข้มข้นของอนุภาคแม่เหล็กในตัวทำละลายที่เหมาะสมในการเตรียมคอมพอสิต และทำการพิสูจน์เอกลักษณ์ด้วย Fourier transforms infrared spectrometer (FT-IR), Scanning electron microscope (SEM) และ Thermal gravimetric analysis (TGA) ผลที่ได้คือ คลอโรฟอร์มเป็นตัวทำละลายที่สามารถนำอนุภาคแม่เหล็กเข้าไปในยางล้อรถยนต์ได้ดีที่สุด ที่ความเข้มข้นอนุภาคแม่เหล็ก 0.04-0.06 g/mL สามารถนำอนุภาคแม่เหล็กเข้าไปใน คอมพอสิตได้ 28.10 เปอร์เซ็นต์โดยน้ำหนัก สำหรับการดูดซับน้ำมันดีเซล คอมพอสิตที่สังเคราะห์โดยใช้คลอโรฟอร์มสามารถดูดซับน้ำมันดีเซลสูงสุดที่ 2.14±0.05 $g \cdot g^{-1}$ ในขณะที่คอมพอสิตที่ถูกสังเคราะห์โดยใช้โทลูอีนเป็นตัวทำละลายสามารถดูดซับน้ำมันเบนซีนได้สูงสุดที่ 2.02±0.08 $g \cdot g^{-1}$ โดยคอมพอสิตทั้งสองชนิดสามารถแยกตัวดูดซับออกจากน้ำด้วยแรงแม่เหล็กได้สำเร็จ

สาขาวิชา ปิโตรเคมีและวิทยาศาสตร์พอลิเมอร์ ลายมือชื่อนิสิต.....

ปีการศึกษา 2555 ลายมือชื่อ อ.ที่ปรึกษาวิทยานิพนธ์หลัก.....

ลายมือชื่อ อ.ที่ปรึกษาวิทยานิพนธ์ร่วม.....

5372498423 : MAJOR PETROCHEMISTRY AND POLYMER SCIENCE
KEYWORDS : WASTE TYRE RUBBER / MAGNETIC NANOPARTICLES / COMPOSITE / OIL SORBENT

PHEERAPHAT NIWASANON : WASTE TYRE RUBBER-MAGNETIC NANOPARTICLE COMPOSITES AS SORBENTS FOR OIL REMOVAL FROM WATER. ADVISOR: ASST. PROF. APICHAT IMYIM, Ph.D, CO-ADVISOR: NUMPON INSIN, Ph.D. 79 pp.

Increases of waste tyre rubber (WTR) and there is not suitable disposal method for this waste. Several tons of WTR degrade slowly. For another environmental issue, oil spill is a worldwide problem. This work used composites between WTR and magnetic nanoparticles (MNPs) as sorbents to remove oil on water surface for easy disposal of sorbent out of water by mean of magnetic separation. The MNPs were synthesized by thermal decomposition of iron-oleate complex in order to control the sizes of MNPs. The WTR/MNPs composites were synthesized in different solvents including *n*-hexane, ethyl acetate, toluene, chloroform, benzene and acetone. Effects of reaction times and concentrations of MNPs in solvent on the properties of the composites were studied. Fourier transforms infrared spectrometer (FT-IR), Scanning electron microscope (SEM) and thermogravimetric analysis (TGA) were used for characterization. It was found that chloroform is the best solvent for incorporating MNPs into WTR at the concentrations of MNPs of 0.04-0.06 g/mL, resulting in the composites with 28.10% w/w of MNPs. The composites prepared using chloroform had highest capacity for diesel sorption at 2.14 ± 0.05 $g \cdot g^{-1}$, while the composites using toluene in the preparation exhibited highest capacity for gasoline sorption at 2.02±0.08 $g \cdot g^{-1}$. Both composites were efficiently removed after used by magnetic separation.

Field of Study : Petrochemistry and Polymer Science Student's Signature .....
Academic Year : 2012 Advisor's Signature .....
Co-advisor's Signature .....

ACKNOWLEDGEMENTS

The author wish to express greatest gratitude to my advisor, Assistant Professor Dr. Apichat Imyim and my co-advisor, Dr. Numpon Insin for their advice, assistance, inspiration, and generous encouragement throughout this research. I would like to extend my appreciation to Assistant Professor Dr. Wanlapa Aeungmitrepirom and Assistant Professor Dr. Fuangfa Unob for their precious suggestions. In addition, the author wishes to express deep appreciation to Assistant Professor Dr. Warinthorn Chavasiri, Dr. Amarawan Intasiri and Assistant Professor Dr. Anawat Pinisakul for serving as the chairman and members of this thesis committee, respectively, for their valuable suggestions and comments. Furthermore, I could be filled with kindness, encouragement, lovely friendship and the good support sincere thanks to all members of EARU (Environmental Analysis Research Unit) and MAT CAT (Materials Chemistry and Catalysis Research Unit). Paticularly, Mr. Nakara Bhawawet, Miss Amornrat Saithongdee, Miss Sumitra khonsa-nga, Miss Natthaporn Warreewat and Miss Padtaraporn Chanhom for their suggestion and assistance.

Appreciation is also extended to Program of Petrochemistry and Polymer Science and the Department of chemistry, Faculty of science, Chulalongkorn University for granting financial support to fulfill this study and provision of experimental facilities.

This thesis could not have been completed without generous help of Miss Sarocha Phumbua for her help. Finally, the author is greatly appreciated to my family and good friend whose names are not mention here for their love, assistance and encouragement throughout my entire education. Without them, the author would have never been able to achieve this achievement.

CONTENTS

Page

Page

Page

Page

Page

LIST OF TABLES

Table **Page**

LIST OF FIGURES

Figure Page

Figure Page

Figure Page

LIST OF ABBREVIATIONS

^{o}C	Degree Celsius
mL	Mililiter
g	gram(s)
Min	Minute
h	Hour
FTIR	Fourier Transform Infrared Spectroscopy
SEM	Scanning Electron Microscope
TEM	Transmission Electron Microscopy
TGA	Thermogravimetric Analysis
UV-VIS	UV-VIS spectrophotometer
VSM	Vibrating sample magnetometer
ICP-OES	Inductively Coupled Plasma-Optical Emission Spectrometer
ASTM	American Society of Testing and Materials
WTR	Waste tyre rubber
TDF	Tyre Derived Fuel
MNPs	Magnetic nanoparticles
SBR	Styrene-Butadiene Rubber
BR	Butadiene Rubber
IIR	Butyl Rubber
WTR/MNPs	Waste Tyre Rubber-Magnetic Nanoparticle Composites

CHAPTER I
INTRODUCTION

1.1 Statement of the problem

The energy is important raw material in manufacture process that is main factor in economy. Therefore, oil is required in many industrial that is rising. Transportation of oil is important because every country has different demanding and source. There are many ways to transport but the main transportation is marine because of low cost. In spite of the fact that oil spill was deliberate releases oil during transportation but may be leak by accident such as the Gulf of Mexico oil spill besides this has minor leak in gas station, garage, house etc. The oil spill not only affect environmental such as oil cover surface that make oxygen cannot into water and has any effect to animal but also human was damaged such as the marine and tourism industries. Therefore, oil spill is the major problem in environments.

So this problem could be solved. There are several methods to eliminate oil spill. The oil spill was eliminated by burning. This method is effective in low wind, beside, this method is occur toxic gas such as carbon monoxide, sulfur dioxide, sulfur trioxide, nitric oxide, and nitrous dioxide. This toxic fume is responsible for a host of environmental problems. Next method is using dispersants to oil spill in order to dissipate oil slicks. This method transfers large amounts of oil from water surface into the water. They will solve problem of oil on water surface but they affect to increase the toxic of hydrocarbon levels. Oil droplets infiltrate into deeper water that affect to kill fish eggs and corals. Another method is using boom and skimmer to eliminate oil slicks. This method is effective but they require the calm waters during the process. Furthermore, the sorbent is one choice to eliminate oil spill because it is complete removal of the oil from the oil spill site, using in everywhere and easy to used. This method is using material to removal of oil spill by absorption and adsorption. The ideal material of sorbent for oil spill include hydrophobicity and oleophilicity, high uptake capacity, high rate of uptake, retention over time, oil recovery from absorbents, buoyancy, and the reusability or

biodegradability of the absorbents. Several absorbents were developed to removal oil but it was eliminated out of water by human. That must use more time and charges.

1.2 Objectives of this thesis

(1) To prepare a new sorbent, waste tyre rubber-magnetic nanoparticle composites,

(2) To studies efficiency of waste tyre rubber-magnetic nanoparticle composites for oil removal,

(3) To apply the synthesized sorbent to remove oil form water.

1.3 Scope of this thesis

Waste tyres rubber (WTR) was applied to study oil spill sorption. Elimination of dispose oil spill and waste tyres by reusing the WTR to absorb oil spill were studied here. In this work, sorbents were prepared by combining WTR and magnetic nanoparticles (MNPs) as composites that are easy to dispose out of water surface by mean of magnetic separation. Ferrite magnetic nanoparticles were synthesized using thermal decomposition of iron (III) oleate in presence of oleic acid surfactant. Parameters affecting incorporation of magnetic particles into WTR e.g. types of organic solvent, time and quantity of magnetic nanoparticles and solvents were optimized to obtain composites with highest oil absorption efficiency while under magnetic control. WTR-magnetic nanoparticle composites were successfully prepared and characterized by scanning electron microscope (SEM), transmission electron microscopy (TEM), infrared spectroscopy (IR) and thermogravimetric analysis (TGA). Oil absorbency measured by ASTM F726 method.

1.4 The benefits of this research

Waste tyre rubber-magnetic nanoparticle composites used to sorbents for oil removal from water by used magnetic force to dispose of sorbents out of system.

CHAPTER II

THEORY AND LITERATURE REVIEW

2.1 Tyre

2.1.1 Composition of Tyre

Tyres are composites rubber compounds consisting of rubber compounds, fabric (nylon), steel, adhesion promoters (cobalt salts, brass on wire, resins on fabric), and processing oils (oils, tackifiers, softeners). Figure 2.1 shows the general structure of a tyre. It is mainly made of rubber that has different properties. The composition of tyres can be varied based on the intended applications and the vehicle they are applied to. Therefore, there are many formula for making tyres. Generally, there are about forty percent by weight of rubber compound and the rest are other substances. The compositions of tyres are listed below.

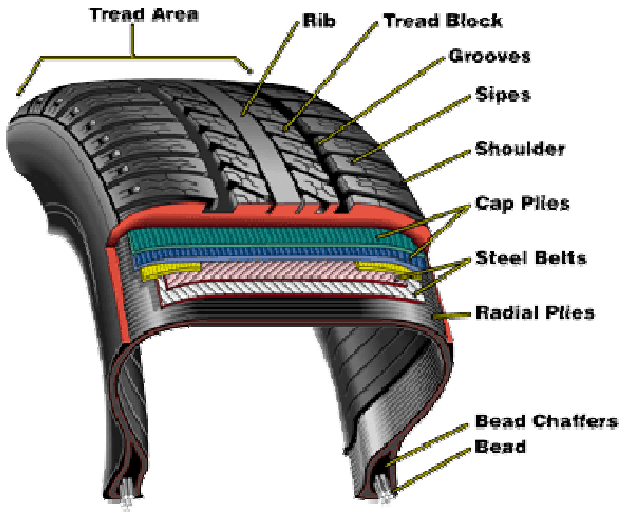

Figure 2.1 Illustration of the structure of a tyre [1].

2.1.1.1 Rubbers

Rubber can be mainly divided into two parts as natural rubbers and synthetic rubbers, each of which contributed equally to tyres used currently [2]. The ingredient ratios of the rubber can be adjusted depending on the applications to obtain specific properties. The parts of side wall and tread containing rubber are responsible

for about 55 percent of the weight of tyre. Rubbers that are widely used are natural rubber, styrene-butadiene rubber and butadiene rubber [2]. Furthermore, there are some special rubbers, such as butyl rubber used in tube tyre due to its suitable properties for used as airtight barrier. For general car tyres, the rubber compound is usually composed of synthetic rubber and natural rubber in the ratio of 4:3 [3].

Natural rubber

Natural rubber or *cis*-1,4-Polyisoprene, of which structure was shown in Figure 2.2, is used as the main component in tyres. The properties of natural rubber are based on the double bond in polymer chain. The natural rubber after some modification can restore the original shape and size and resist to organic solvents, heat and ozone. However, the oxidation reaction can affect the rubber properties in that the rubber is less flexible and less stable. The natural rubber has so low stability that it will deform and flow following shape of container. Therefore, the rubber has to go through the conversion process and be cured by vulcanization.

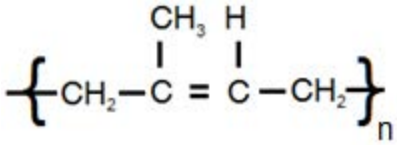

Figure 2.2 Structure of *cis*-1,4-polyisoprene

Synthetic rubber

Styrene-butadiene rubber (SBR), butadiene rubber (BR) and butyl rubber (IIR) were the main components of synthetic rubbers. There are different properties in each type of synthetic rubbers.

Styrene butadiene rubber (SBR) is also known as a copolymer that consists of 23% of styrene monomer and butadiene monomer of about 77%. The outstanding features of SBR are high abrasion resistance and adhesion properties. Styrene makes the process of forming of tyre occur more easily. SBR is also more resistant to swelling in polar solvents. However, the disadvantages of SBR are that it has low resistant to ozone, UV and high heat buildup. The structure of SBR was shown in Figure 2.3.

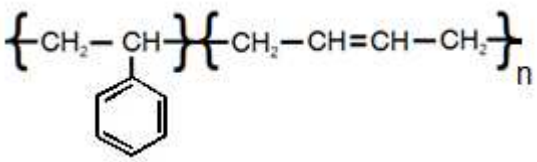

Figure 2.3 Structure of styrene-butadiene rubber

The higher percentage of SBR affects in the decrease in flexibility, tensile strength, tear resistance, abrasion resistance, sunlight resistance, ozone resistance, oxygen resistance and heating resistance than natural rubber.

Butadiene rubber (BR) has high resistance to abrasion, low heat buildup, and low rolling resistance. BR is usually used to blend with natural rubber or SBR for tyre sidewalls and treads because of the special properties of high elasticity at low temperature. However, BR has unique and advantageous properties but it cannot be used solely because it is difficult to compound. The structure of BR was shown in Figure 2.4.

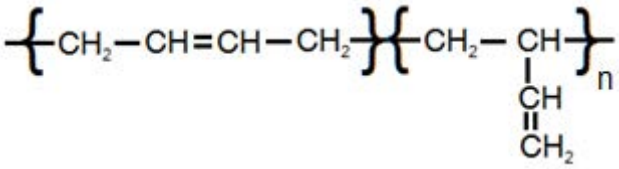

Figure 2.4 Structure of Butyl rubber

Butyl rubber (IIR) is the copolymer between monomer of isobutylene and a small amount of isoprene, which included in order to preserve the good properties of isobutylene. Due to low levels of unsaturation of this rubber, it is resistant to oxidation, ozone, high-pressure steam and good electrical insulator. However, butyl rubber is very low gas permeability, so the major product of butyl rubber is used to produce as tyre innerliners. The structure of Butyl rubber was shown in Figure 2.4.

2.1.1.2 Additive for rubber tyre

Vulcanization is process of reaction between rubbers and vulcanizing agents. The vulcanizing agents are sulfur complexes or other equivalent curatives.

Vulcanizing agents of appropriate amount could be used to form crosslinks between each polymer chain at the temperature above the melting points of vulcanizing agents. The vulcanization increases durability of the materials. Vulcanized materials have superior mechanical properties to the native ones for instance resistance to heat, oxidizing environments and various solvents. However, the materials are less sticky. A wide variety of products are made from vulcanized rubber including the tyres, shoes, soles, hoses, and hockey pucks.

Figure 2.5 Example of vulcanization process.

Uncured natural rubber is sticky and easily deformed at high temperature, but brittle at low temperature. Chemical structure of natural rubber is mainly long polymer chains, and the molecular chains can move independently. Vulcanized natural rubbers have crosslink that prevent moving of polymer chains. Stretched rubber was deformed but without stress, so it can return to original shape [4].

Activators [5] are chemicals or mixture of chemicals, which function to increase the performance of the catalyst (accelerators) and increase the rate of the polymerization reaction. Activators increase the cross-link density of the rubbers due to the fact that cross linking reactions of diene rubbers took place faster. Activators that are most commonly used in the rubber industry, including ZnO and stearic acid, can form complexes with accelerators. ZnO is an activator to activate sulfur vulcanization in order to reduce the vulcanization time. Figure 2.6 shows the evolution of mono-, di-, and polysulfides crosslinks with cure time in the case of natural rubber vulcanization.

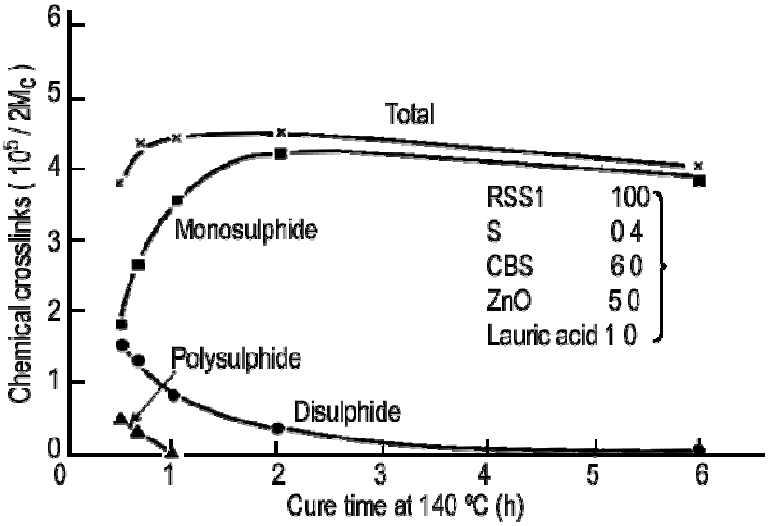

Figure 2.6 Chemical crosslinks vs. cure time of NR [6].

Accelerators are chemicals used to accelerate reaction in processing of rubber. Small quantities of accelerators, such as monomeric polysulfides, are added to rubbers in order to increase speed of vulcanization and reduce the time of stabilization process. Accelerators interact with rubber to produce polymeric polysulfides which help with the crosslinking in rubber. Some examples of accelerators are diphenyl guanidine, N-tert-butyl-2-benzothiazole sulphenamide, cyclohexylthiophthalimide, morpholin-4-yl morpholine-4-carbodithioate, and thiuram.

2.1.1.3. Other additives

Plasticizers (aromatic oils)

Plasticizers help with the processability and mixture process of the rubbers because they can increase the flexibility, the elastic behaviour of vulcanisate. Plasticizers also facilitate the incorporation and dispersion of high loads of filler that was added to improve hot-air resistance and enhance properties when applied at low temperature. Examples of plasticizers are aromatic oils.

Filler

Filler materials are solid additives, such as carbon black, calcium carbonate, silica, and clay. Small particle size of fillers may be added to the rubber or latex in bulk in order to improve properties or to reduce production costs.

Antidegradants

There are many types and functions of antidegradants. One type of antidegradant is added to inhibit oxidation reaction. The common chemicals for antioxidants include quinolines, phenolic stabilizers and phenylenediamines, for example IPPD (N-Isopropyl-N'-phenyl-p-phenylene diamine), TMQ (2,2,4-Trimethyl-1,2-dihydroquinoline), and BHT (2,6-Di-tert-Butyl (p-cresol)). Antioxidants are consumed during product are used. Antioxidants may also migrate with vulcanizing agent.

2.1.2 Tyre Management

Waste tyre rubbers (WTR) accumulate of several millions tons per year that make a large environmental problem. Almost waste tyre rubbers have been discarded in landfills and WTR is still tyre structure because it is durable and low levels of moisture. Furthermore it is little degradation in several years. The innovations of disposal have been developed, recycled, and energy recovered. Moreover, alternated fuel that uses tyres through combustion in industries. However, combustion process generates gaseous pollutants as carbon monoxide, sulfur dioxide and solid waste or ashes, which must be securely disposed to reduce environmental impacts. So several researches had shown methods to reduce environmental pollutants as depicted in Figure 2.7.

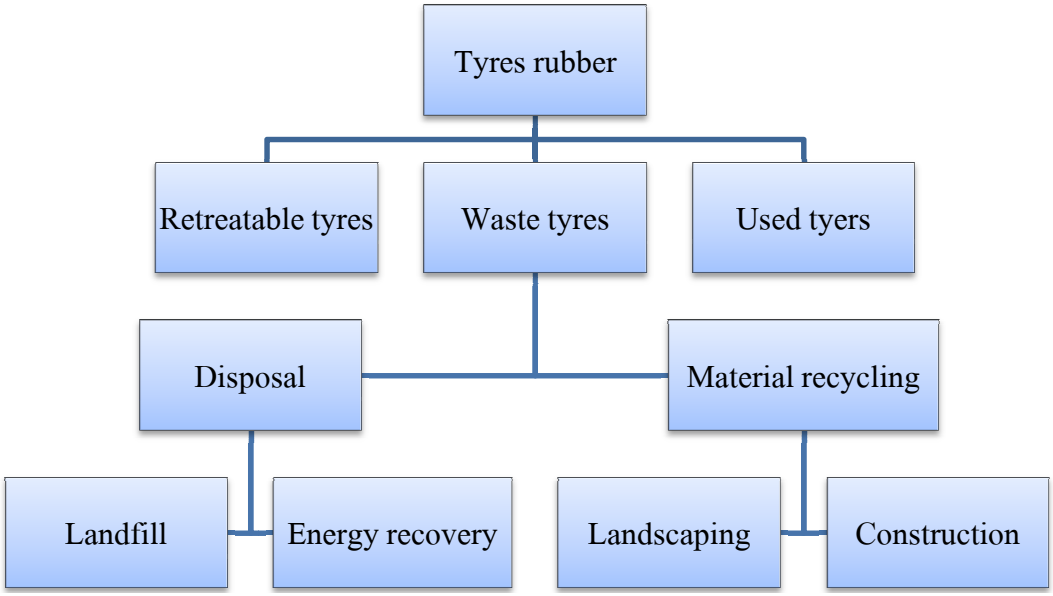

Figure 2.7 Schematic diagram showing the life-cycle of tyres and tyre management.

Energy Recovery

Energy recovery maybe call tyre derived fuel (TDF). This process uses waste tyre rubber inenergy generator. For example; it is uased in cement production. Its heat value is more than coal.

Landfilling

The current waste tyres rubber is still end at landfills. All landfills accept waste tyres and require costly fee because tyres are difficult to manage. That must use large region to keep tyres because it is hard to compact. Waste tyres are usually resized before landfilling in order to reduce region to keep. Tyre will be banned from landfills in EU Member States. Waste tyres must be separated from other waste materials and stored at a licensed location.

Material recycling

This process is attention in research to recycling products which decrease waste tyres and increases value of waste tyres. Almost products must be undergone several processes in order to high quality products. The major process is to resize and to separate waste tyres. That must require several technologies to process it which requires cryogenic processes to resize due to the fact that tyres have elasticity properties. The finished waste tyre rubbers have diameters about 0.5 to 10 mm. That can be used for playground, artificial turfs, modified concrete [7] and roads that use to mix with asphalt [8]. The separation process is used to separate steel and textiles out off tyres which use principle of density and magnetic by vibration density and magnetic separators. The resize scheme is presented in Figure 2.8.

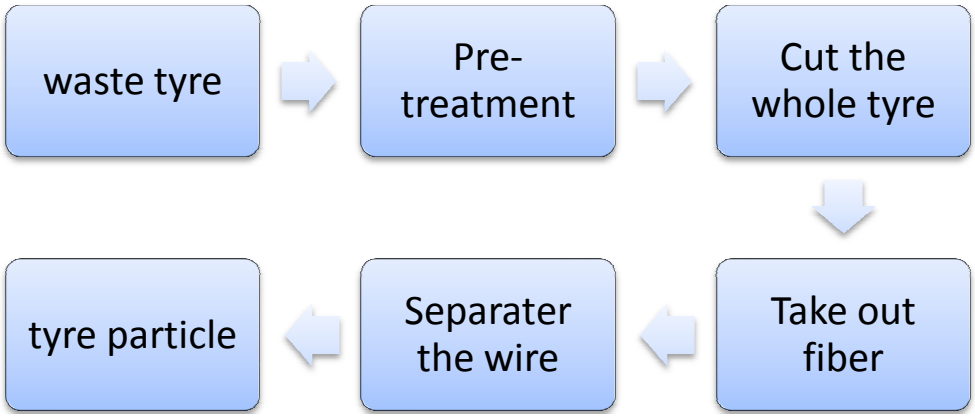

Figure 2.8 Schematic diagram showing the resize of tyres.

2.2 Contamination of oil spill

Oil leaks affect to pollution of environment that occurs by several causes. . Mainly three ways are air, land, and water.

Oil contamination in air

Air does not contaminate by oil directly, but the volatile organic compounds (VOCs) in oil can release in air. In general gasoline can evaporate easily. The volatile is 1,2,4-trimethylbenzene (TMB) which is a major product in a petroleum refinery distillation or about 40% that is C9 aromatic. Almost refineries add C9 fraction to gasoline [5]. Furthermore, burning oil makes carbon dioxide and carbon monoxide cause toxic in air.

Oil Contamination in land

Oil can be dispersed on land. There are many garages that used to repair car, motorcycle, truck, etc. Waste oil is essential to the process. Furthermore, an accident about fuel truck results large contamination in land. Oil covers over soil that make water cannot insert to soil. Absorption, transferring and replacement of oil contaminated in soil are hard to resolve this problem which is costly to remove oil. There are several methods to solve this problem such as steam/air stripping, encapsulation, chemical treatment, bioremediation, etc [9].

Oil Contamination in water

There are many ways of contamination of oil in water which mainly occurs by human activity particularly marine transfer of oil. The oil spill is discharged of liquid petroleum to environment. Oil spill spreads to another area by ocean current that is hard to pick up and clean. There are several processes to remediate oil contamination. Oil spills clean up procedures must be considered to use mixed methods to lower risk to environment.

2.3 Decontamination of Oil Spill

Oil spill is a large problem that remains effects to the environment. There are several methods to decontaminate oil spill. Each method can dispose oil in different fields. The types of methods are as follows:

2.3.1 Physical Methods

These environmental friendly techniques use a physical principle to separate oil spill.

2.3.1.1 Booms and skimmer [10]

Oil spill is mainly recovered by booms and skimmer. Booms are equipment to use for oil contamination on surface water which floats on water. Moreover, booms creep to contain oil. Function of boom is helping to confine or change the direction of oil that is used in conjunction with skimmer. Some kinds of booms have fire-resistant properties. The function of booms is depicted in Figure 2.9.

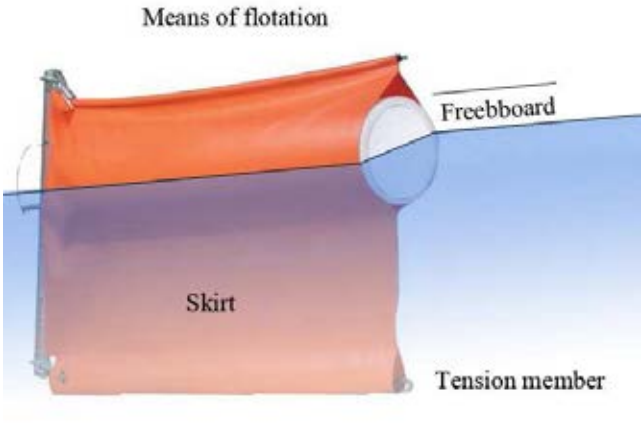

Figure 2.9 An illustration of the components of boom [11].

The commercial booms include

1) a means of flotation : to float of the boom

2) a freeboard : to keep oil from leak on the top of the boom

3) a skirt : to protect oil from under the boom

4) a tension member : to support a preparing of boom

There are many kinds of boom. Booms are usually used to protect oil from spreading due to easy disposal and treating; in addition, it also protects bays and beaches from oil. Particularly, biologically sensitive areas are important to ecosystem. The basic kind of booms is fence, curtain booms and external tension member booms.

A skimmer is equipment to dispose oil from the water's surface. The simple property of oil is low density than water so that oil floats on the water's surface. The oil is separated from the water easily by skimmer.

2.3.1.2 Thermal Method

Thermal method usually using in-situ burning is a high effective way for oil elimination on water's surface that is removed over 90% of oil. Carbon product is

released by carbon dioxide about 90-95%. While combustion that was generating by-product of toxic such as carbon monoxide, sulfur dioxide, nitrogen dioxide, polynuclear aromatic hydrocarbons(PAHs), and particulates (dust, soot, etc.)

2.3.1.3 Sorbents

Sorbents are materials for disposal of oil from water's surface or land by either absorption, or adsorption, or both. Application of suitable sorbent for final elimination of oil spills, boom and skimmer cannot go to these areas and primary disposal for very small spills. Sorbent has efficient to remove oil on water's surface that is less than boom and skimmer to dispose. There are many kinds of sorbent that can be synthetic or natural materials such as synthetic sorbents, natural organic sorbents and natural inorganic sorbents. Each material is used mechanism which in general term can be divided into absorption, adsorption or both.

There are materials that have different behaviors in sorption process. Absorbents are sorbent materials that can pick liquid up and distributed through its structure. Therefore, the materials swell. That is usually applied more than 50 percent of usage. Adsorbents are materials or modify material that may be coated with liquid on surface involving capillaries and pores. However, the recoverability is important in economics.

Sorbents can be divided as synthetic and natural sorbents. That is a different method to remove oil from water's surface and recovery.

Natural sorbents are divided two groups. Organic sorbents for example peat moss, wool, feathers, wood, hay, sawdust etc. The advantage is environmental friendly and they can degrade in the environment. Inorganic sorbents for instant perlite, clay, vermiculite, glass wool, and sand. These are durable, but it is difficult to recover.

Synthetic sorbents are mainly made from polypropylene and another is polyurethane, polyethylene, etc. The mostly used are branched and linear polymers. That is easy to recover and durable. Moreover, it is cheap than some nature sorbents.

2.3.2 Chemical Methods

The chemicals are used to treat oil spill in order to help environment by recovery or sorption. These techniques involve several methods to use chemicals that are modified to aid for oil removal. The methods are divided as follows:

Dispersants

These are chemicals designed to dispread oil spill by spraying to oil slicks, for example Miyabi Dispersants [12]. Dispersants help to dispread the oil slicks which rapid than natural dispersion. The chemicals include surfactants, solvent compounds that use to break oil slick into droplets by emulsification. They possess molecule's hydrophilic properties and lipophilic properties which help to attach oil slick by decreasing interfacial tension of water and oil [12]. It helps to remove oil from the water's surface in addition to natural processes for example ocean currents and waves [13]. Dispersants are used with light to medium weight oils expected crude oil because they do not disperse as well. Dispersants must be used immediately for oil spill before the light oils have evaporated. There are many factors to be used dispersants effectively which include temperature, water salinity, ocean current, and other. However, dispersants have not been used extensively because it makes environmental effects in long term [10]. The droplets have dispreaded to ocean floor and it is toxic to marine life.

Gelling Agents (Solidifiers)

These chemicals are used with oil spill by reacting with oil in order to deform to rubber-like solids [13]. That can be used with small to large oil spill. The gelled oil is easy to remove than oil slick by using nets, suction equipment, or skimmers, and etc. In general gelling agents are used in calm ocean. In addition, they may be used in wave's condition. There is problem in these chemical, as high volume of oil spill that is difficult to remove because it has the large size.

2.3.3 Biological Methods

This methods use biological agents to remediate oil spill. That is usually called “biodegradation”. In nature, there are many kinds of microorganisms to degrade oil for example bacteria, fungi, and yeast. This takes a long time to remove oil from water’s surface by biodegradation. Furthermore, there are many factors in biodegradation to degrade oil. Thus this method is not widely applied to oil spill.

2.3.4 Natural Methods

This method takes a long time for oil removal. The processes can occur by evaporation, photooxidation, biodegradation, etc. Each process will eliminate oil spill that depends on conditions. Evaporation can occur for light weight oil. Photooxidation occurs when sun light shins to oil that can react with oxygen.

2.4 Absorbents for Oil Spill Cleanup

2.4.1 Absorbent Forms [14]

There are various shapes and forms of absorbents. It depends on composition and physical properties of materials. Their forms are boom, pad, pillow, roll, sweep, and particulate.

2.4.2 Ideal properties of sorbents

Expected properties of sorbents are presented in Table. 2.1

Table 2.1 Ideal properties of oil sorbents

Properties	Descriptions
High hydrophobicity	Sorbents must be high hydrophobicity in order to like oil more than water which can absorp oil.
High uptake capacity	This property is more interesting because quantity of sorbents is decreased.
High rate of uptake	The sorbents must be able to reach quickly in order to decrease oil decontamination on water with high efficiency.

Properties	Descriptions
Buoyancy	Floating absorbent is important to recovery process in order to conveniently recover, particularly when sorbent is left over ocean the oil is less viscous.
Reusability or biodegradability and recoverability of the sorbent oil	This property is important to decrease cost in oil decontamination.

2.5 Effect of liquid to rubber

2.5.1 Chemical effect

The effect of chemical occurs by additives or chemicals. Rubber and liquid react when receiving suitable temperature. The almost chain polymer is crosslinked or being scission in atmosphere. The reaction makes to change physical properties as follows;

2.5.2 Physical effect

Physical properties can be changed by 2 types. There are absorption and extraction because each process affects to behavior of rubber which increase or decrease volume of sample rubber.

Absorption

Absorption makes swelling rubber and increase volume. The volume is expands to limit depending on type of rubber and solvent, time, temperature, shape, etc. That affects to physical properties such as hardness, elongation, tensile strength, etc.

Extraction by solvent

Additive, plasticizer, antioxidant can be released from rubber resulting in decreasing volume (called shrinkage).

There are parameters to describe and predict the effect of rubber and solvent.

- The rule “like dissolves like”

- The solubility parameter
- Aniline point
- The elastomer compatibility index (ECI)

2.5.3 Like Dissolves Like

The polar solvent likes to dissolve with polar polymer and non-polar solvent like to dissolves with non-polar polymer.

The rule of thumb “like dissolves like” is used with linear polymer for example nonvulcanize rubber, plastics, thermoplastic elastomers. But vulcanized rubber cannot use “like dissolves like” because it swells in solvent such EPDE elastomers swells in mineral oil due to the fact that EPDE is hydrocarbon polymer and mineral oil is hydrocarbon solvent. Therefore, the structure was showed properties of rubber dissolves with solvent.

2.5.4 Solubility parameter

This principle is simple to predict liquid and solid force, exceptionally polymer. Solubility parameter is used to know swelling of vulcanizing rubber in solvent. This property is important for application.

Molecules of solute and solvent are compatible and co-exist when dissolved. Rate of solubility depends on molecular weight, temperature, etc. Solvent can be mixed with solute that depends on interaction forces. The interaction forces of different molecules are more important than those of same molecules that can be co-exist. The interaction force can predictby cohesive energy density (CED). That is energy of vaporization per molar volume. The equation of CED is expressed as;

$$CED = \frac{E_{coh}}{V} = \frac{\Delta H_v - kT}{V}$$

where E_{coh} is the energy of cohesion, ΔH_v is the heat of vaporization, V is the molar volume, T is the temperature. The unit of CED is cal/cm^3 and MPa (SI units).

The solubility parameter can be found by Hildebrand equation (see Table 2.2) The solubility parameter can be derived by the following expression.

$$\delta = \sqrt{CED} = \frac{\rho \sum G}{M}$$

where δ is the solubility parameter ($cal^{1/2}/cm^{3/2}$ and $MPa^{1/2}$), G is the molar attraction constants (see Table 2.3), M is the molecular weight.

Table 2.2 Hildebrand Solubility Parameters [15]

Solvent	$(cal/cm^3)^{1/2}$	$MPa^{1/2}$
n-Hexane	7.24	14.9
n-Heptane	7.40	15.3
Diethyl ether	7.62	15.4
1,1,1 Trichloroethane	8.57	15.8
Cyclohexane	8.18	16.8
Amyl acetate	8.50	17.1
Carbon tetrachloride	8.65	18.0
Xylene	8.85	18.2
Ethyl acetate	9.10	18.2
Toluene	8.91	18.3
Tetrahydrofuran	9.52	18.5
Benzene	9.15	18.7
Chloroform	9.21	18.7
Trichloroethylene	9.28	18.7
Methyl ethyl ketone	9.27	19.3
Acetone	9.77	19.7
Diacetone alcohol	10.18	20.0
Ethylene dichloride	9.76	20.2
Methylene chloride	9.93	20.2
Pyridine	10.61	21.7
Morpholine	10.52	22.1
Dimethylformamide	12.14	24.7
n-Propyl alcohol	11.97	24.9

Solvent	$(cal/cm^3)^{1/2}$	$MPa^{1/2}$
Ethyl alcohol	12.92	26.2
Dimethyl sulphoxide	12.93	26.4
n-Butyl alcohol	11.30	28.7
Methyl alcohol	14.28	29.7
Propylene glycol	14.80	30.7
Ethylene glycol	16.30	34.9
Glycerol	21.10	36.2
Water	23.50	48.0

Table 2.3 Molar attraction constants at 25°C [16]

Group	molar attraction constant (G)
$-CH_3$	214
$-CH_2-$ (single bonded)	133
-CH<	28
>C<	-93
$CH_2=$	190
-CH=(double bonded)	111
>C=	19
CH=C-	285
-C=C-	222
Phenyl	735
Phyenylene (o,m,p)	658
Ring (5-membered)	105-115
Ring (6-membered)	95-105
Conjugation	20-30
H	80-100
O (ether)	70

Group	molar attraction constant (G)
CO (ketones)	275
COO (esters)	310
CN	410
Cl single	270
Cl twinned as in $>CCl_2$	260
Cl triple as in $-CCl_3$	250
Br single	340
I single	425
CF_2 ,CF_3 (in fluorocarbons only)	150,274
S sulphides	225

The solubility parameter of small molecule can be found by CED or molar attraction constants but large polymeric molecule must be tested by using different solubility parameter solvents. The result is plotted to find the best solvent to select the solubility parameter. Polymer with vulcanizing cannot dissolve but it swells and it can be chosen a solvent following the highest of graph (see Figure 2.10).

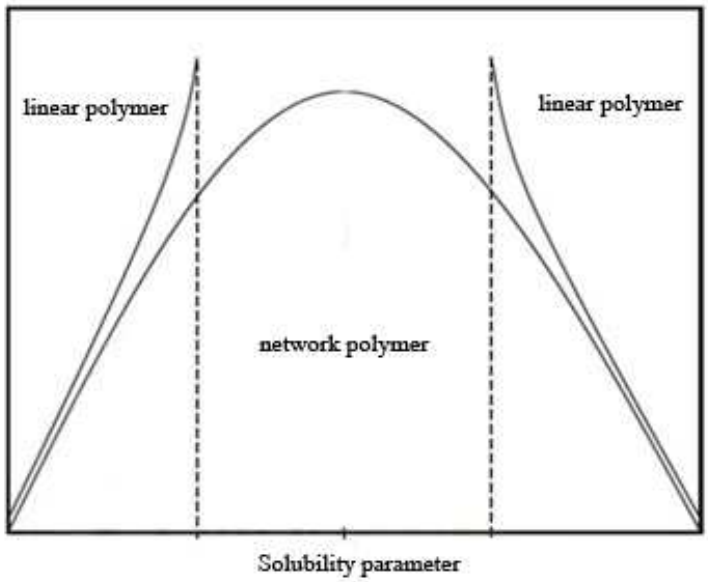

Figure 2.10 Illustration of the equilibrium swelling as a function of solubility parameter for linear and cross-linked polymer [17].

Hansen solubility parameters [18]

The solubility parameter of polar and hydrogen bonding system is calculated by polar, hydrogen bonding, and dispersive. The equation is shown.

$$\delta_t^2 = \delta_d^2 + \delta_p^2 + \delta_h^2$$

where δ_t is the Hansen solubility parameter, δ_d is the energy from dispersion forces, δ_p is the energy from dipolar intermolecular force, δ_h is the energy from hygrogen bonds.

Böttcher Equation $\delta_p^2 = \frac{12108}{V^2}\frac{\varepsilon-1}{2\varepsilon+n_D^2}(n_D^2+2)\mu^2$ cal/cm^3

Beerbower Equation $\delta_p = \frac{37.4(\mu)}{V^{\frac{1}{2}}}$ MPa^{½}

2.5.5 Swelling by solvent [19]

Crosslinked elastomer swell in a good solvent this is a basic phenomenon [20]. The cross-linked elastomer expand volume when solvent molecules penetrated. A good solvent for elastomer is predicted by solubility parameter. Moreover, the kinetics of solvent entering to elastomer is limited by diffusion. That rate depends on type of solvent and polymer, temperature, pressure, etc. The swelling can be reversible by squeezing and decreased pressure that affect to swelling. The driving force of solvent and resistance of the polymer network to expansion should balance. The solvent molecule is drawn in polymer chain, but it is not soluble because the crosslinks develop a resistance to expansion. Furthermore, the swelling depends on solvent molecules penetrating to cross-linked elastomer that was shown in Figure 2.11. The equilibrium of swelling can be calculated following this formula.

$$V_s = \frac{w_0}{\rho_2} + \frac{w_s - w_0}{\rho_1}$$

where V_s is the equilibrium volume after swelling, w_0 in the initial mass of the elastomer, w_s is the equilibrium swollen mass, ρ_1 is the density of solvent, and ρ_2 is the density of polymer.

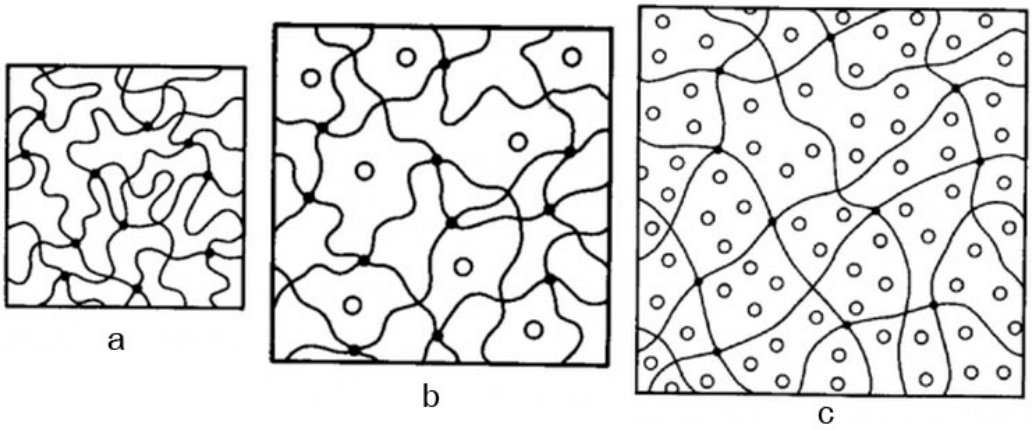

Figure 2.11 Swelling of cross-linked elastomer after penetration of solvent molecules [19].

The regular theory of solution predicts a bell shaped curve that is shown in Figure 2.12. So solvent uptake depends on solubility parameter of solvent and polymer when matched thus a maximum in polymer swelling occurs.

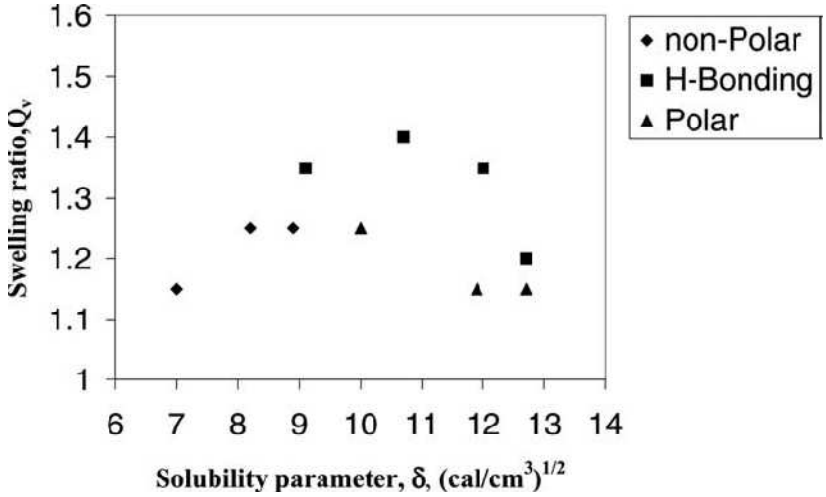

Figure 2.12 A bell shaped curve of solubility parameter in polymer swell [21].

2.6 Magnetic Properties

Paramagnetism

Dipole moments of paramagnetic material preferentially align by rotation when the material was exposed to an external magnetic field and arrange in the same direction. However, the dipole moment is less than the highest possible value. The behavior of materials respond less in the same direction with a magnetic field is called

“paramagnetic” [22]. Alignment of magnetic dipole is lost when an external magnetic field is removed.

Ferromagnetism

Ferromagnetic materials exhibit a spontaneous magnetization. Spontaneous magnetization occur when electrons in 3d-obital arrange themselves in same direction [22]. In addition, these materials magnetized easily when exposed to strong magnetic field. These materials remain magnetized after the removal of an external magnetic field. Magnetic susceptibility of these materials is higher than that of paramagnetic materials. Ferromagnetic materials lose their magnetic properties when heated to curie point; on the other hand, when cooled down, they exhibit ferromagnetic properties again. Examples of ferromagnetic materials are Iron (Fe), Cobalt (Co), Nikel (Ni), and Gadolinium (Gd).

Antiferromagnetism

This property can be regarded as a special case of ferromagnetism. Magnetic dipoles of the antiferromagnetic materials arrange themselves in opposite direction in magnetic field, resulting in the net dipole moment of zero. Examples of these materials are Manganese (Mn) and Chromium (Cr).

Ferrimagnetism

This magnetic property is also regarded as a special case of ferromagnetism in that there is alignment of magnetic dipoles but there are some alignments in opposite direction. Therefore, these materials exhibit spontaneous magnetization. These properties are found in some ionic compounds, such as ceramic, oxides, or more complex forms. A group of materials called “ferrites (AB_2O_4)”, such as magnetite (Fe_3O_4) is known for its ferrimagnetism. A ferrimagnet is consisted of two magnetic sublattices (A and B), and oxygen ions are mediated for exchange interactions between the spinning of A and B sublattice. Ferrimagnetism and ferromagnetism have similar properties such as remanence and spontaneous magnetization.

Superparamagnetism

This behavior occurs by a reduction of the magnetic material domain into a single domain state in a particulate. Superparamagnetic materials behave like paramagnetic in that they have no permanent magnetic moment, but they respond strongly to an external magnetic field the same magnitude as ferromagnetic and ferromagnetic materials do. More detail of this property will be discussed in Section 2.8.

2.7 Magnetic nanoparticles

Magnetic nanoparticles (MNPs) are interesting in a wide range of research fields including biomedicine, magnetic resonance imaging, catalysis, magnetic fluids, etc. There are several methods developed for MNPs synthesis. The MNPs are highly stable under conditions that promote the formation of independent particles. The particle size of a single magnetic domain are around 35-120 nm [23]. Each nanoparticle shows superparamagnetic properties. However, the periods of time of stability are an unavoidable problem. Nanoparticles tend to agglomerate because small size of magnetic particle is associated with the high surface area. The metallic nanoparticles are highly active to oxidation in air. As a result, nanoparticles will loss of dispersibility and superparamagnetism in some periods of time. For several applications that need stable MNPs, the surfaces of particles have to be protected by organic or inorganic species such as surfactant [24], polymers[25], silica [26], carbon [27], etc. These protecting coating layers can increase the period of the nanoparticles.

2.8 Superparamagnetic [28]

The superparamagnetic character is shown when temperature is higher than the blocking temperature. The blocking temperature depends on the instrumental measuring time, the size of the particles, the effective anisotropy constant, and the applied magnetic field. The behavior of superparamagnetic is a large magnetic moment that shows a fast response when exposed to magnetic fields even though the materials

possess magnetic moment with negligible remanence and coercivity. The magnetization curve of these materials shows no hysteresis loop.

The character of superparamagnetism comes from the reduction in sizes of magnetic materials. Most of bulk magnetic particles have multidomain structures. Domains are separated by domain walls. The domain walls are controlled by the balance between the magnetostatic energy (ΔE_{MS}), which is proportionally to the volume, and the domain-wall energy (E_{dw}) of the materials. A well-isolated single-domain particle exhibits superparamagnetism. The single-domian state occurs by reduced particle size to below the critical volume. The critical diameter lies in a range of few nanometers depending on type of materials and their anisotropy energy terms. The single-domain state is reached when $\Delta E_{MS} = E_{dw}$, that means $D_c \approx 18\frac{\sqrt{AK_{eff}}}{\mu_0 M^2}$; where D_c is the critical diameter of a spherical particle; A is the exchange constant Natural rubber; K_{eff} is the anisotropy; constant μ_0 is the vacuum permeability, and M is the saturation magnetization. The supperparamegnetic character occurs when the diameter of magnetic particle is less than the critical diameter (D_c).

2.9 Ferrofluids

Ferrofluids are superparamagnetic colloidal suspensions dispersed by organic or aqueous media. W. C. Elmore first found ferrofluids in 1938 [24]. Ferrofluids sometimes are referred to as magnetic fluids or magnetic colloids as shown in Figure 2.13. The surfactant is coated on particles by attraction with Van der Waals and electrostatic forces. The particles are randomly dispersed that can be solved by Brownian motion. The magnetic moments of ferrofluid are proportional to the volume because the particles have single domain and can be regarded as point dipoles. The relation between magnetic moment and size of the particles are formulated as,

$$m = \frac{\pi}{6} \times M_s D^3;$$

where M_s is the saturation magnetization, and D is the diameter of magnetic particles. The magnetic interaction, which is of interest in many applications and research, can be calculated by this following formula.

$$U_{dd} = \frac{\mu_0}{4\pi r_{12}^3}[\vec{m}_1 \cdot \vec{m}_2 - 3(\vec{m}_1 \cdot \hat{r}_{12})(\vec{m}_2 \cdot \hat{r}_{12})];$$

Where U_{dd} is the magnetic interaction, $\vec{m}_1$, $\vec{m}_2$ is the magnetic moments of magnetic particle and $\hat{r}_{12}$ is the distance of center to center distance between magnetic nanoparticles.

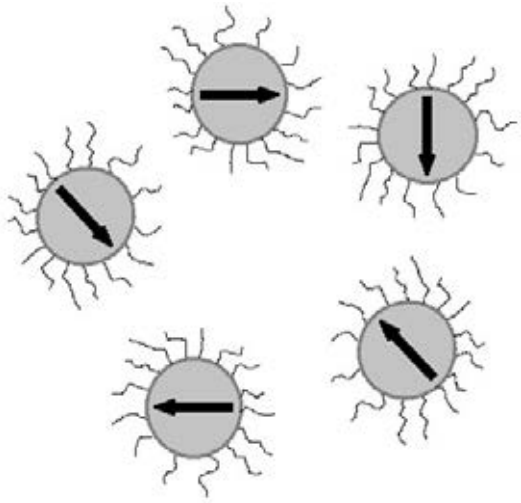

Figure 2.13 Schematic diagram of a ferrofluid where nanoparticles are coated with a surfactant.

2.10 Iron oxides

There are several forms or allotropes of iron oxides. The interesting forms are magnetic iron oxides such as magnetite (Fe_3O_4), maghemite (γ-Fe_2O_3) and hematite (α-Fe_2O_3). Moreover, the other related ferrite structures whose formula are $MO{\cdot}Fe_2O_3$ (where M is Mn, Co, Ni, Cu) are also of interest. Magnetite, maghemite, and hematite are very important in current innovation such as bio-sensor [29], chemotherapy [30], biomedical applications [31].

2.10.1 Magnetite (Fe_3O_4) [32]

Magnetite adopts the inverse spinel structure as shown in Figure 2.14. The unit cells of the inverse spinel are face-centered cubic of O^{2-} ions framework and iron ions atoms occupy interstitial sites. The trivalent ions occupy both tetrahedral and octahedral sites; while divalent ions occupy octahedral sites. The chemical formula of magnetite can be written as $Fe^{III}(Fe^{II}Fe^{III})O_4$.

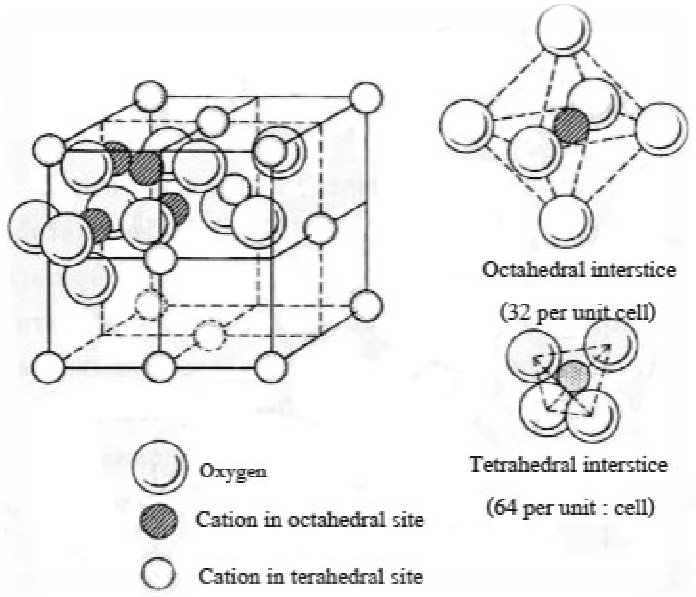

Figure 2.14 Spinel structure

Magnetite is classified as ferromagnetic materials. This material is the oldest known magnets [32]. The Fe (III) ions in tetrahedral site are aligning antiparallel to those in octahedral sites below 851 K. The dynamic disorder of divalent and trivalent iron distribution in octahedral sites changes to a long-range order with an orthorhombic structure when the temperature is below 120 K.

The stoichiometric of magnetite is not commonly obtained due to the fact that divalent iron may be replaced by other divalent ions [32]. The flexibility of oxygen framework causes Fe(II) ions can be replaced with other divalent ions.

2.10.2 Maghemite (γ-Fe_2O_3)

The maghemite has the same structure as magnetite but maghemite has the trivalent of Fe in the two sublattices. The unit cell of maghemite contains $21\frac{1}{3}$ of Fe^{III} ions, 32 of O^{2-}, and $2\frac{1}{3}$ vacancies. The vacancies exist in octahedral sites. The nature of precursor, the crystallite size and the amount of Fe^{II} are related to the extent of vacancy ordering. The magnetic property of maghemite is also ferrimagnetism. The ferrimagnetism occurs by unequal distribution of ions in tetrahedral and octahedral sites. Maghemite is usually used in recording media due to its stability and low prices.

2.11 Literature review

2.11.1 Polymer sorbents for oil removal

Ceylan *et al.* [33] studied macroporous polymeric material as sorbent in oil spill cleanup. The sorbent was synthesized using butyl rubber (BR). The sorption capacity of BR is 15-23 g/g for crude oil and petroleum products. This sorption capacity is higher comparing to a nonwoven polypropylene (PP), which is widely commercial sorbent, of which sorption capacity is 10-16 g/g. BR sorbent can be reused by squeezing, and its continuous sorption capacity is 7.6 g/g in each cycle. The sorbent can be reused for about 3 times for crude oil sorption. Furthermore, BR sorbents can be removed polycyclic aromatic hydrocarbons (PAHs) such as as acenaphthene and pyrene, from seawaters. This sorbent is a better alternative to PP sorbents in that it can improve the efficiency of oil sorption and reusability of the sorbent.

Karakutuk and Okay [34] studied the preparation of macroporous organogels that was made by Butyl rubber, cis-polybutadiene (CBR) and styrene–butadiene rubber (SBR). The crosslinker, sulfur monochloride (S_2Cl_2), was used in the gel preparation. Organogel network was composed of large pore of 10^1-$10^2\mu m$ in diameter. Benzene crystals were used as templates for synthesis at -18°C. The networks of CBR and SBR exhibited regular pores but PIB had irregular pores with wide distributed pore

sizes. The efficiency of sorption was tested with crude oil, gasoline, diesel, fuel oil and olive oil. The sorption can be continuously reused for two to three times. The results of sorption capacities of CBR and SBR gels for crude oil and olive oil are 33–38 g/g and 24–27 g/g, respectively.

Lin *et al.* [35] studied the oil absorption of composite materials between polypropylene (PP) fiber and waste tyre powder. The composites were used to recover spilled engine oil. PP sorbent has a large, rapid oil sorption capacity, but it has elasticity limited for repeated uses. The material with elasticity which is tyre powder, and tyre can be used repeatedly without losing its efficiency. However, tyre powder absorbs less oil and more slowly than PP. The composites were developed by mixing PP fiber and tyre powder. The results showed that the composites can be used repeatedly for at least 100 times. The composite materials maintained a constant oil sorption of 4.0 g/g. Also, these composites are low cost.

Although there are several types of oil sorbents, but from the literature reviews mentioned above, polymer-based sorbents were widely studied. Polymer sorbents are interesting oil sorbents because polymer is hydrocarbon-based materials similar to oil. Polymer and oil will be highly compatible. Moreover, the polymer sorbents have high durability, which is the property suitable for oil sorbent. However, polymers have different capacities depending on physical and chemical properties of polymer sorbents themselves.

2.11.2 Use of waste tyre rubber

Oil removal application

Lin *et al.* [36] studied capacity of waste tyre to adsorb motor oil. Waste tyre of the size of 20 mesh can be adsorbed 2.2 g of motor oil. The cleaning process affected the capacity of sorbents and the capacity of sorbents was ranked in the order of *n*-hexane cleaning> water cleaning > un-cleaned > dishwashing liquid cleaning > seawater cleaning. Waste tyre powder is reusable for more than 100 times while it remains the same efficiency. The results also indicated that the oil sorption efficiency

increased as the waste tyre powder size and temperature decreased. For the effect of cleaning water, the results found that seawater yield higher efficiency of sorbents than fresh water.

Koutsky *et al.* [37] reviewed the materials used for oil sorption. The material has been overlooked including reclaimed recycling rubber particles. Old tyres have advantage property in that there have slightly greater density than water. The newer cryo-milling techniques which used liquid nitrogen to break the old tyres to fine particulates of 30-50 mesh in diameter. The reinforcing fibres in the rubber matrix can be separated out easily. Rubber particles rapidly absorbed oil and form a viscous cohesive mass readily. Furthermore, Rubber particles can be floated on water surface and be easily picked up.

Aisien *et al.* [38] studied to use recycled rubbers as sorbents due to enormous available scrap tyres. The rubber particle sizes and temperature of absorption affected the absorption capacity of rubber particle. The absorption capacities in oil-polluted fresh waters and marine waters were the same. The attendant survival of aquatic organisms, fish in this case, was investigated to observe the effects of oil pollution. The survival time of the fish depended on the dissolved oxygen concentration and amount of rubber particle. The absorption was not hindered by water due to the fact that the rubber is hydrophobic.

Wu *et al.* [39] reused the waste tyre rubber (WTR) for oil sorbent using graft copolymerization-blending with 4-tert-butylstyrene (tBS) for the development of WTR. The WTR, which obtained from Zhejiang Lvhuan Rubber Powder Engineering Co. Ltd, was de-vulcanized before used. The initiator and crosslinker are divinylbenzene (DVB) and benzoyl peroxide (BPO), respectively. The maximum absorbency for crude oil diluted with toluene of 60/40 feed ratio is 24.0 g/g.

From the literature, we found that WTR can be used as promising oil sorbent due to that fact that WTR is hydropobic and has buoyancy, making it can be recovered easily. Besides, uses of WTR are the reuse of tyres resulting in the decrease of waste.

Several researches developed WTR to be good sorbents by chemical and physical processes.

Other applications

Kershaw *et al.* [40] studied the ability of treated ground rubber for the sorption of benzene and o-xylene from water containing aromatic hydrocarbons. The ground rubber can adsorb at equilibrium capacities is 1.3 and 8.2 mg/g of benzene and o-xylene, respectively in batch tests. For the packed bed column, it takes average time of 15 min to get 40% utilization rate.

Kim *et al*.[41] studied the sorption tests of tyre rubber with organic compounds and investigated the sorption capacity. The effects studied were types of organic compounds, ionic strength, pH, ground tyre particle size, and temperature of sorption. The partition coefficient of m-xylene was the highest, followed by ethylbenezene, toluene, trichloroethylene, 1,1,1-trichloroethane, chloroform, and methylene chloride. However, the diffusion coefficients did not correlate well with the physical and chemical properties.

Torrado *et al.* [42] studied on using used tyre rubber (UTR) prepared to carbonaceous adsorbents (CAs) for the adsorption of organic and inorganic solutes in aqueous solution. UTR was treated by chemical treatments with HCl, HNO_3 and NaOH aqueous solutions and heat treatment at 900 °C for 2 h in N_2 atmosphere (H900). The adsorbents were tested for adsorption of phenol, *p*-aminophenol, *p*-nitrophenol, and *p*-chlorophenol and of chromium, cadmium, mercury and lead in aqueous solutions. The development of porosity in this treatment is very poor. However, H900 is the only CA with a well developed porosity of mainly in the regions of meso and macropores. For this CA, the adsorption of all the adsorptives is greater than other samples. UTR and the UTR-derived products were characterized by N_2 adsorption at -196 °C to study the texture, and FT-IR spectroscopy was used to characterize the oxygen surface groups and pH of the point of zero charge (pHpzc). Particular for *p*-nitrophenol and

p-chlorophenol is on the one side and on the other side for mercury and lead. Adsorption is much higher for mercury and lead than for the remaining adsorptives.

2.11.3 Magnetic nanoparticles

Sun *et al.* [43] prepared magnetite nanoparticles by partial reduction coprecipitation method. However, the nanoparticles were not stable in exposure to oxygen. Magnetic properties were lost in 2 months. The maghemite has better chemical stability than magnetite, and it has comparable magnetic properties. The magnetite was transformed to maghemite by aeration oxidizing of acidified magnetite nanoparticles aqueous suspension. The maghemite nanoparticles are 13.5 nm in diameter.

Song *et al.* [44] studied the synthesis of monodisperse MNPs using thermal decomposition method. The precursor is $Fe(oleate)_3$ in 1-octadecene. The MNPs are devised into two shapes, quasi-cubical and spherical, with similar sizes.

Hyeon *et al.* [45] prepared monodisperse MNPs using iron pentacarbonyl and oleic acid to generate iron-oleic acid complex by thermal decomposition method. This approach can be used to prepare the MNPs size is range 4 – 16 nm.

Park *et al.* [46] developed the method for preparation of monodisperse MNPs. The reactants are non-toxic and inexpensive. The process is generalized. The reaction was large scale and without a size-sorting process. MNPs were synthesized by iron chloride and sodium oleate. The particle size ranged from 8 to 11 nm and showed superparamagnetic behaviour at high temperatures.

In conclusion, several magnetic nanoparticles have been synthesized by various methods. However, in some methods, size, shape, distribution and uniformity of particle are comparatively poor due to physical and chemical properties of MNPs. Furthermore, aggregation of MNPs depends on sizes and surfaces, and can be prevented by coating with some surfactants. Therefore, when magnetic particle are desired to be monodisperse in size, the proper methods should be considered.

CHAPTER III

EXPERIMENTALS

3.1 Instruments

The instruments used for measurements and characterization in this thesis are shown in Table 3.1

Table 3.1 List of instruments

Instruments	Manufacture: Model	Purpose
Thermogravimetric analyzer (TGA)	Perkin Elmer: Pyrisl	Thermal stability of the materials
Scanning Electron Microscope (SEM-EDX)	JOEL: JSM-5800 LV	Imaging of the WTR and composites and elemental analysis
Transmission Electron Microscope (TEM)	JEOL: JEM-2100	Determinations of size, and shape of MNPs
UV-VIS spectrophotometer	Hewllet Packard: 8453	Determinations of MNPs concentration
Fourier Transform Infrared Spectrophotometer (FT-IR)	Nicolet Instruments Technologies: Impact 410	Determinations of functional group
Inductively Coupled Plasma-Optical Emission Spectrometer (ICP-OES)	Thermo: model iCAP 6500	Determinations of MNPs concentration

3.2 Chemicals

All chemicals used in this research are listed in Table 3.2.

Table 3.2 List of chemicals

Chemicals	Suppliers	Grade
Iron(III) chloride anhydrous	Fisher scientic	analytical grade
Sodium hydroxide	Merck	analytical grade
Oleic acid	Merck	analytical grade
Ethanol	Merck	analytical grade
n-Hexane	Carlo Erba	analytical grade
Toluene	Merck	analytical grade
Chloroform	Lab-Scan	analytical grade
Benzene	Merck	analytical grade
Acetone	Reagent chemical	analytical grade
Ethyl acetate	J.T. Baker	analytical grade
1-Octadecene	Aldrich	technical grade
Diesel	shell	commercial
Gasoline	shell	commercial

3.3 Experimental procedures

3.3.1 Preparation of reagents

Sodium hydroxide solutions

1.2 M Sodium hydroxide solutions were prepared by dissolving the 0.96 g of sodium hydroxide in 10 mL DI water.

Iron (III) chloride solutions

0.4 M of Iron (III) chloride solutions were prepared by dissolving the 1.29 g of iron (III) chloride anhydrous in 10 mL of DI water.

3.3.2 Synthesis of MNPs

The MNPs were synthesized via thermal decomposition following the method reported by Jongnam Park et al. [46], which is divided into two steps. First, Iron-oleate complex was prepared by reaction between iron chloride and sodium oleate. Sodium oleate was prepared by mixing sodium hydroxide solution with oleic acid. Then, iron (III) chloride solution and sodium oleate were mixed and dissolved in a mixture solvent consisting of 16 mL of ethanol, 12 mL of distilled water, and 28 mL of *n*-hexane. The solution was heated at 70 °C and kept at this temperature for 4 h. The upper organic layer contains the iron–oleate complex when the reaction was completed. The upper organic layer was washed three times with 6 mL of distilled water. After washed, the organic layer was put under reduced pressure in a rotary evaporator to evaporate off *n*-hexane. The resulting iron-oleate complex was in a waxy solid form. Next step, to synthesize iron oxide nanoparticles, 3.6 g of the iron-oleate complex and 0.57 g of oleic acid were dissolved in 20 g of 1-octadecene. The reaction mixture was heated to 320°C with a constant heating rate of 3.3°C min^{-1}, and kept at this temperature for 1 h. The conditions for the whole process were summarized in Table 3.3. The resulting solution containing the MNPs in 1-octadecene was cooled to room temperature, and 100 mL of ethanol was added to the reaction mixture to precipitate out the MNPs. The MNPs were separated by centrifugation and kept in *n*-hexane. For the effect of time for synthesizing of MNPs, reaction time of the step hold at 320°C (Step 4 in Table 3.3) was varied from 30 min to 2 h.

Table 3.3 Conditions for each step for synthesis of iron oxide nanoparticles

Step	Temperature (°C)	Time (min)	Feed
1	50	15	Vacuum
2	50	60	
3	320	81	Nitrogen gas
4	320	60	
5	160	5	Air
6	160	120	
7	25	30	

3.3.3 Preparation of WTR

Waste tyre rubber (WTR) powder was received from Union Commercial Development Co. Ltd. (Samut Prakan, Thailand). It was sieved to collect the WTR of particle sizes between 50 – 60 mesh using an ASTM wire sieve. The obtained WTR was pre-treated by washing separately with solvents i.e. acetone, benzene, chloroform, ethyl acetate, *n*-hexane, and toluene in order to eliminate impurities and undesired substances that might interfere sorption efficiency. After that, the WTR was directly dried in an oven at 100°C for 3 h before use.

3.3.4 Composites preparation

Composites of WTR and magnetic nanoparticles (MNPs) or WTR/MNPs were prepared by immersing WTR in MNPs solution. The preparation conditions were optimized by varying immersion time, types of organic solvent and concentration of MNPs.

3.3.4.1 Effect of solvent

The composite WTR/MNPs was synthesized by immersing 1.0 g of WTR in 10.0 mL of 0.02 g/mL MNPs suspended in different organic solvents (acetone, benzene,

chloroform, ethyl acetate, hexane, and toluene). The mixture was stirred continuously by means of a magnetic stirrer for 4 h. The solvent was evaporated using a rotary evaporator. The remaining WTR solid composite was washed several times with hexane to remove all excess MNPs that might attached at the surface of WTR. Finally, the WTR/MNPs composite was dried in an oven to eliminate remaining hexane.

3.3.4.2 Effect of time

The composites were synthesized using the same method as described above in 3.3.4.1, but time was varied for 2, 4, 24, and 120 h.

3.3.4.3 Effect of concentration

The composites were synthesized using the same method as described above in 3.3.4.1, but the concentrations of MNPs were varied in the range of 0.01 - 0.06 g/mL. According to the results obtained from the previous sections, only chloroform and ethyl acetate were used as solvent.

3.3.4.4 Effects of quantity of WTR

The composites were synthesized using the same method as described above in 3.3.4.1, but the amount of WTR was varied in the range of 0.25 – 1.50 g.

3.4 Characterization of MNPs

3.4.1 Imaging of magnetic particles by TEM

MNPs were characterized by Transmission Electron Microscopy (TEM). The image of MNPs showed magnetic particle size, shape, and distribution of magnetic particles.

3.4.2 Testing magnetic property by VSM

The magnetization of MNPs and the composites was analyzed using Vibration Sample Magnetometer (VSM). The magnetization was measured by applying magnetic field ranging from -10000 to 10000 G for each sample.

3.4.3 Identification of the structure of MNPs by XRD

The XRD pattern was determined using X-ray diffractometer (XRD). The characterization and identification of crystalline structures were done by comparing the diffraction pattern of scattered X-rays from the samples with the standard from database. XRD pattern was recorded in the two-theta range of 20 to 80 degree.

3.4.4 Determination of dispersed MNPs in solvents.

The dispersed MNPs are important to the syntheses of composites. MNPs originally dispersed in *n*-hexane were evaporated by rotary evaporator in order to eliminate *n*-hexane. The solvent (*n*-hexane, ethyl acetate, chloroform, benzene, toluene, and acetone) was added to the dried MNPs, and the dispersions were sonicated for 20 min before further used.

3.5 Characterizations of composite

3.5.1 Determination of MNPs in composites

The UV-VIS spectrophotometer was used to determine the percentage of MNPs that was washed out with *n*-hexane from composites in order to find percentage of magnetic particles in composites. The excess MNPs were eliminated by washing several times with *n*-hexane. Concentration of MNPs was determined using a calibration curve between absorbance at 450 nm and concentration of MNPs [47]. The wavelength for measuring the absorbance was chosen to be 450 nm to avoid the interfere by organic surfactants,

3.5.2 Characterization by FTIR

A Nicolet Fourier Transform Infrared Spectrophotometer, Model Impact 410 (Nicolet Instruments Technologies, INC. WI, USA) was used to record FTIR spectra of each composite and WTR. The infrared spectra were recorded between 400 to 4000 cm^{-1} in Attenuated Total Reflectance (ATR) mode.

3.5.3 Thermal analysis by TGA

The thermograms of each composite were measured using thermogravimetric analyzer: pyrisl (Perkin Elmer). Each sample was tested under the condition of 20°C/min heating rate over a temperature ranging from 25 to 800°C under nitrogen atmosphere to determine the weight loss that can indicate the composition in WTR and composite.

3.5.4 Characterization by SEM

The scanning electron microscope (SEM) was used for analysis of the morphology composites which can imply the presence of MNPs embedded into WTR matrix. The distribution of magnetic particles was studied by elemental mapping method using Energy dispersive X-ray (EDX) spectroscope equipped with the SEM.

3.5.5 Stability of MNPs in composite

3.5.5.1 Analysis of the quantity of MNPs in composites

The stability of MNPs in composites affects the uses of these composites because MNPs may leave out of the composites upon using and re-using. Quantity of MNPs was measured by Inductively Coupled Plasma Optical Emission Spectroscopy (ICP-OES). Before the analysis, 0.1 g of samples was soaked in mixture of 6 mL of hydrochloric acid and 4 mL of nitric acid for 24 hr and heating until WTR composites was degraded.

3.5.5.2 Analysis of the quantity of MNPs in oil

Quantity of MNPs in oil was measured using ICP-OES. Digestion was used to prepare sample. In this method, 20 mL of oil after sorption process was soaked in a mixture of 6 mL of hydrochloric and 4 mL of nitric acid for 24 h, and then the mixture was heated until became black solid. Finally, the black solid was diluted with 2% nitric acid and heated to dissolve. The hot solution was filtered with filter paper and membrane filter. The solution was adjusted volume using 2% nitric acids in composites. The excess MNPs were eliminated by washing several times with *n*-hexane. Concentration of MNPs was determined using a calibration curve between absorbance at 450 nm and

concentration of MNPs. The wavelength for measuring the absorbance was chosen to be 450 nm to avoid the interfere by organic surfactants,

3.6 Oil sorption capacity tests

American Society of Testing and Materials (ASTM) F726-99 method was referenced for oil sorption capacity tests. The sorption experiment was performed by weighing 0.1 g of WTR/MNPs sample into a sintered glass crucible No. 3 and afterward placing in a 50 mL beaker containing 20 mL of diesel or gasoline oil. Then the crucible was taken out, cleaned by tissue paper and placed on a suction flask. Excess oil was removed by suction pump. The initial and final weights of crucible and WTR/MNPs sample were recorded. All of the oil sorption was tested at 25 ^{o}C. The oil sorption capacities were calculated from the equation [48]:

$$Q = \frac{m_0 - m_s}{m_s} \quad (3.1)$$

where Q is weight uptake of oil, m_s is the initial weight of the WTR/MNPs sample and m_0 is the weight of the sample after sorption.

The effect of sorption time was also studied by varying the contact times of 10, 20, 30, 60, 90,120 and 180 min. All experiments were done in triplicate.

3.7 Composite sorbent reusability

The reusability of composite was evaluated by placing 3 g of the composite WTR/MNPs, which was synthesized by chloroform, into a sintered glass crucible No. 3. And afterward the crucible was placed in a 50 mL beaker containing 20 mL of diesel. After an absorption period, the crucible was taken out, cleaned by tissue paper and placed on a suction flask. Excess oil was removed by suction pump. And the adsorbed oil was removed by a weight pressing on the composite WTR/MNPs. The initial and final weights of crucible and WTR/MNPs sample were recorded. This experiment was performed at 25 ^{o}C.

3.8 Synthetic sample

The experiment was performed by pouring 0.5 mL of crude oil in a 50 mL beaker containing 20 mL of DI water and afterward 0.1 g of WTR/MNPs sample immersed in the beaker. Then WTR/MNPs sample was taken out of beaker by permanent magnetic. The final weight of WTR/MNPs sample was recorded. All of the oil sorption was tested at 25 ^{o}C. The effect of sorption time was also studied by varying the contact times of 10, 20, 30, 60, 90,120 and 180 min.

CHAPTER IV
RESULTS & DISCUSSION

Composites of magnetic nanoparticles (MNPs) and waste tyre rubber were prepared to study as oil sorbents. The composites were synthesized in following solvents, acetone, benzene, chloroform, ethyl acetate, *n*-hexane, and toluene. Quantities of MNPs incorporated into WTR depend on solvent types. This research also studied the influences of time and concentration of MNPs. Besides, composites were studied for sorption of diesel, gasoline and crude oil.

Part I Preparation and characterization of MNPs and WTR/MNPs composite

4.1 Morphologies of Magnetic nanoparticles

The morphologies of MNPs were characterized by Transmission electron microscopy (TEM). MNPs of difference particle size are shown in Figure 4.1. The diameter and size distribution of MNPs depend on the time of crystalline growth. MNPs synthesized with the growth time of 30 min were large size distribution (Figure 4.1a.). At this growth condition, some particles were bigger than other particles. When we increases the growth time of MNPs to 1 h and 2 h, the size distributions are quite monodisperse. With the growth time of 2 h, MNPs were cubic structure (Figure 4.1c.) Particularly, at the growth time of 1 h, MNPs have the diameter about 8-10 nm and narrow size distribution, which is the most suitable for preparation of composites.

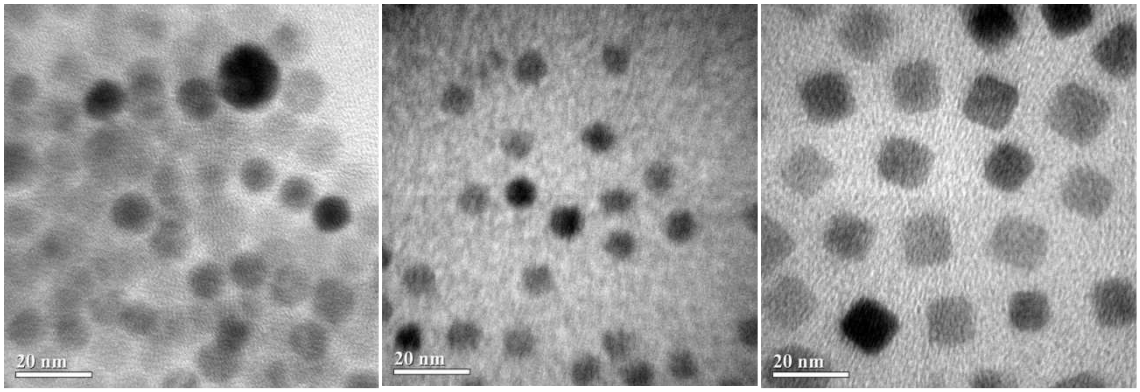

Figure 4.1 TEM images of MNPs with the growth time of (a) 30 min (b) 1 h and (c) 2 h

4.2 The dispersibility of magnetic nanoparticles

The MNPs can be dispersed in organic solvents with different dispersibility and stability. MNPs could be easily dispersed in benzene, chloroform, *n*-hexane, and toluene. The magnetic dispersions appeared as black solution that had not agglomerated MNPs at the bottom of the bottles. In contrast, MNPs in ethyl acetate and acetone appeared as blown solution and had agglomerated magnetic at the bottom of the bottles. MNPs dispersed with less stability in acetone than ethyl acetate because acetone is higher polar than ethyl acetate. The appearances of these dispersions are shown in Figure 4.2.

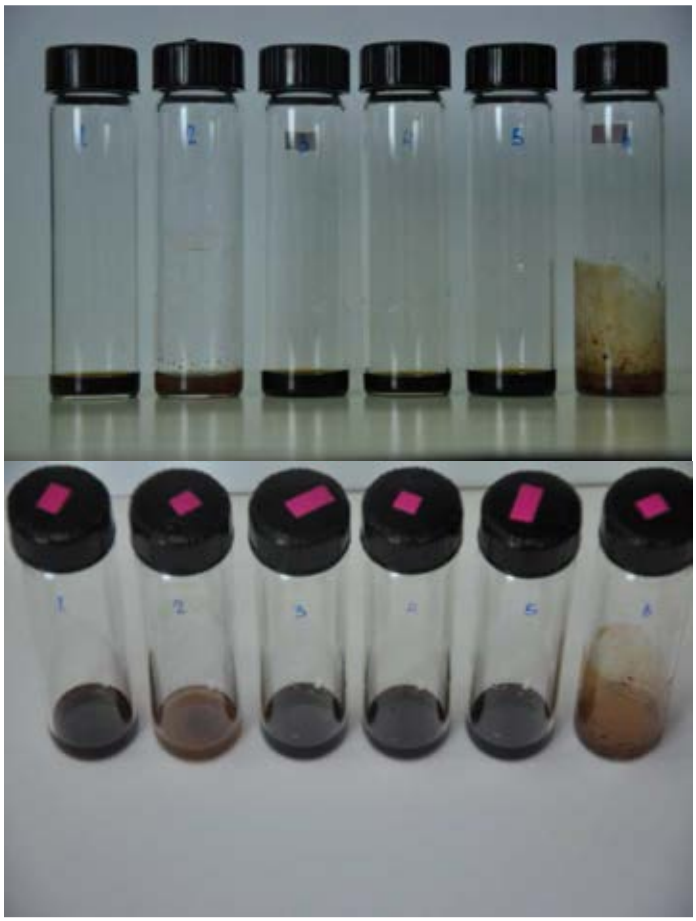

Figure 4.2 The dispersibilities of MNPs in *n*-hexane (1), ethyl acetate (2), toluene(3), chloroform(4), benzene(5), and acetone(6)

4.3 The swelling of WTR in solvents

This effect swelling of WTR in solvents was studied to find the suitable solvents for preparation of composites. Each solvent used in this research projects causes the swelling of WTR due to fact that solvents can be transferred into WTR. The solvent molecules can be diffused between polymer chains. MNPs were inserted to WTR according to the swelling effect of solvents. The results of swelling were obtained by immersing WTR in solvents for 1 h to 24 h and measured the increase weight of the WTR. The results are shown in Figure 4.3.

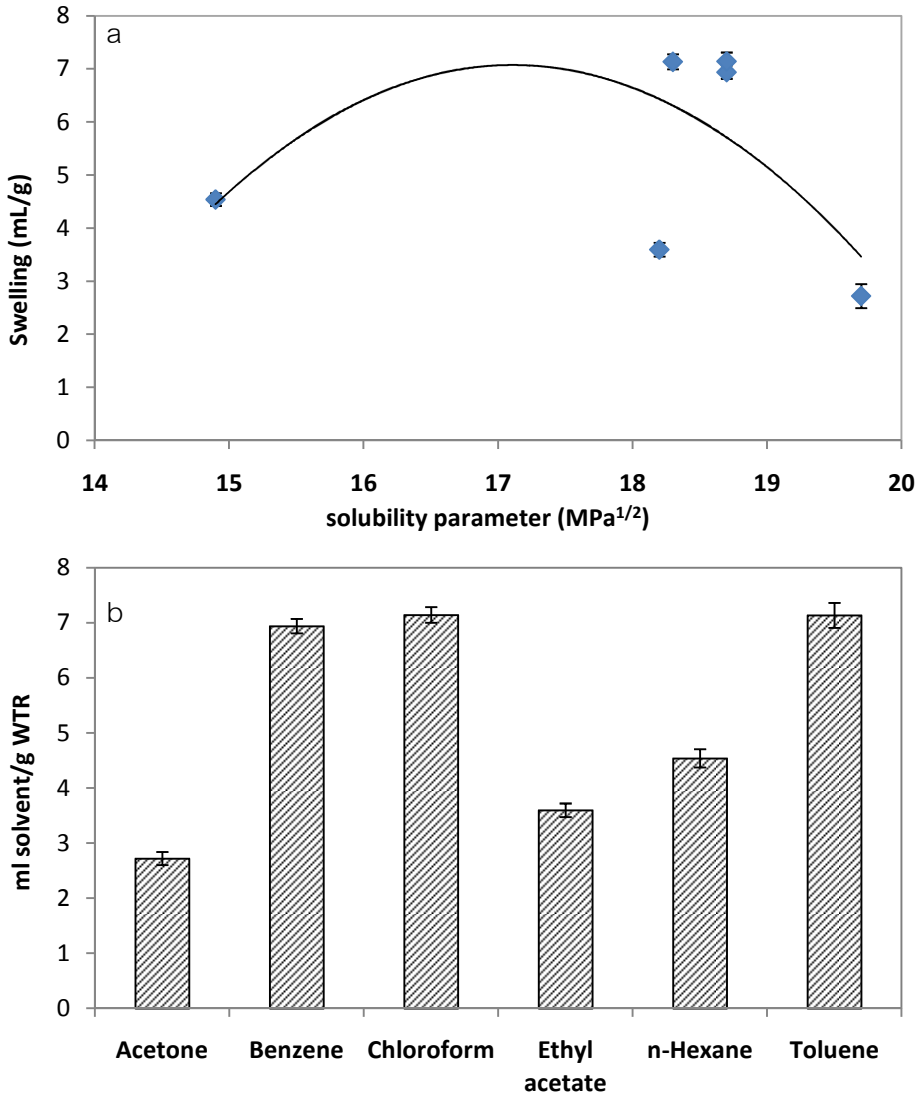

Figure 4.3 Swelling of WTR in solvents in response to changes in solubility parameter (a) and types of solvent (b).

The difference in the solvent uptake value due to swelling followed the polarity and solubility parameter of solvents. The swelling of WTR was shown in a bell shaped curve of solubility parameter. According to regular solution theory predicts a maximum in the plot of swelling versus solubility parameter that the maximum should occur at the solubility parameter of the polymer [21]. Therefore, the solubility parameter of WTR should be about 18 $MPa^{1/2}$ [34]. First group of solvents including hexane, toluene, chloroform, and benzene has similar swelling due to low polarity. Moreover, chloroform yielded the highest swelling comparing with other solvents likely due to its higher relative density [49]. Benzene, chloroform, and toluene have high level of swelling due to the fact that their solubility parameters are close to WTR. Ethyl acetate and acetone gave low level of swelling because of of their high polarity. The changes in swelling time from 1-24 h gave similar results, indicating that the swelling reach equilibrium within 1 h. Furthermore, the bonds between rubber chains during vulcanization should affect the solvent uptake value [50]. The higher flexibility of the crosslink should yield higher solvent uptake.

4.4 Factors affecting the formation of composites

There are many factors in the synthesis of the composites, such as solvent types, duration of synthesis, concentration of MNPs, quantity of WTR, etc. These effects were studied in this work.

4.4.1 Effects of solvent types

The effect of solvent types in synthesized composites was studied. Composites were prepared by mixing MNPs solution with WTR, and stirring by magnetic stirrer. The mixtures were then evaporated in order to remove solvent by rotary evaporator. The excess MNPs were eliminated by washing several times with hexane. The MNPs incorporated into the composites were determined using the calculations from the concentrations of eliminated MNPs measured by UV-VIS spectrophotometer.

The concentration of MNPs measured using absorbance of MNPs solution at 450 nm. The percent by weight of MNPs in each solvent was shown in Figure 4.4.

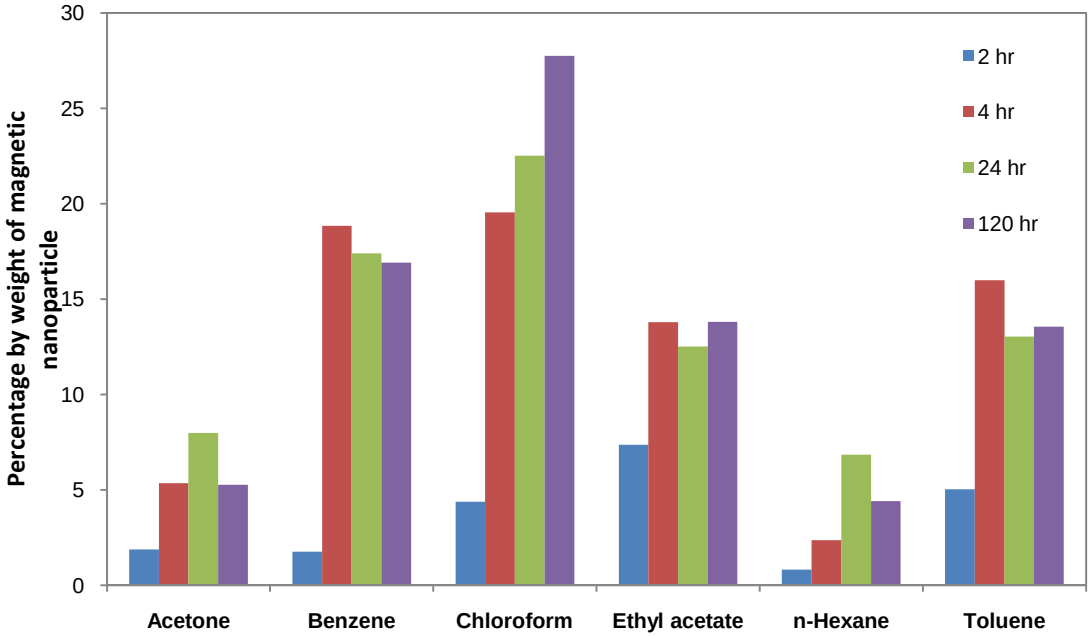

Figure 4.4 Effects of types of solvent to the weight percent of MNPs in the composites

The results showed that the weight percent of MNPs in WTR was the highest when the composites were prepared using chloroform as solvent. The result indicated that MNPs can be embedded into WTR using various solvents but some solvents promote the incorporated of MNPs than others. The weight percent of MNPs incorporated into WTR was in the decreasing order from benzene, toluene, ethyl acetate, *n*-hexane, and acetone. The MNPs added into WTR followed the same trend with the swelling effect shown in Figure 4.3.

Properties of solvents are used to explain the results. Hydrocarbon solvents include benzene, toluene, and *n*-hexane. WTR has good sorption of hydrocarbon solvents. Besides, sorption of WTR depends on solubility parameter. Solubility parameters of chloroform (18.7 $MPa^{1/2}$), benzene (18.7 $MPa^{1/2}$), and toluene (18.3 $MPa^{1/2}$) are similar, resulting in the high percent of MNPs loaded in composites prepared using these solvents. The other group is polar solvents including ethyl acetate and acetone. The weight percent of MNPs in the composites prepared from these polar solvents was

lower than composites prepared in hydrocarbon solvents. Weight percent of MNPs in composites are related to WTR swelling. WTR swelled the most in chloroform which was also the best solvent that allow the penetration of MNPs into WTR.

Moreover, the effect of incubation time to the weight percent of MNPs in the composites was studied by varying the incubation time to 2, 4, 24, and 120 h. It was found that weight percent of MNPs in the composites increased when incubation time increased. At time of 4 h, the loading of MNPs reach saturation in all solvent systems except chloroform, of which MNP percent increased continuously upon the increase of incubation time. The reason for higher ability of chloroform is likely due to the fact that chloroform can disperse MNPs well, has highest density, and its polarity and solubility is close to WTR. Therefore, chloroform is most suitable solvents for the syntheses of the composites.

4.4.2 Effects of concentration of the MNPs to the synthesized composites.

Concentration of the MNPs was studied. The WTR/MNPs composites were prepared by mixing MNPs dispersed in various solvents and WTR. The mixture was stirred using a magnetic stirrer for 4 h and then the solvents were evaporated off using a rotary evaporation. Excess MNPs were washed off using hexane. Concentration of MNPs was detected by a UV-VIS spectrophotometer. In this work, solvents were divided into two groups. First group is the solvents that can disperse MNPs well (i.e. chloroform, benzene, toluene, and hexane). The other group is the solvents with less MNPs dispersibility (including ethyl acetate and acetone). After the preliminary screening, chloroform and ethyl acetate were selected because both have the highest percent loading of MNPs of each solvent group. Results of effect concentrations of MNPs on the loading of MNPs in composites using chloroform and ethyl acetate as solvents was shown in Figure 4.5.

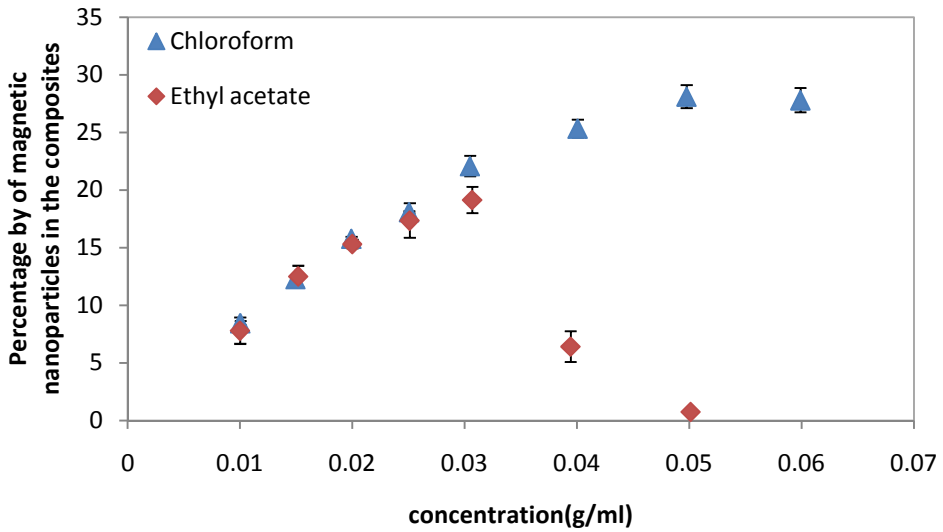

Figure 4.5 The effect concentrations of MNPs on the loading of MNPs in composites using chloroform and ethyl acetate as solvents.

From the study of the effect of concentration of MNPs in solvents (chloroform and ethyl acetate), it was found that increasing concentration of MNPs have direct relation with weight percent of MNPs loaded into WTR before the saturated loading. The loading of MNPs from the synthesized composites using chloroform was increased as the concentration of MNPs was increased until the weight percent reached ~25%. On the other hand, in case of ethyl acetate as solvent, it was found that the percent loading of MNPs increased and reached the highest loading at the concentration of MNPs at 0.03 g/mL. Interestingly, the percent loading of MNPs decreased when higher concentration of MNPs was used. The reason for this phenomenon is likely due to the fact that MNPs are less dispersed in ethyl acetate and trend to agglomerate more in this solvent. When the MNPs agglomerated, magnetic particle size was increasing and became so large that they cannot penetrate molecular chains of WTR. From this observation, we concluded that chloroform is the most suitable solvents studied for the preparation of composites. Moreover, the suitable range of MNPs concentration is 0.04 – 0.06 g/mL in which the highest percent loading of MNPs in composites will be obtained.

4.4.3 Effects of the quantity of WTR to MNPs loading in the composites.

The factor of WTR quantity was of interest and studied because the quantity of WTR could strongly affect to the quantity of MNPs embedded into WTR and we would like to find the most suitable WTR quantity for the preparation of the composites. The experimental set up was similar to the experiment in Section 4.4.2, but the concentration of MNPs was kept at 0.03 g/mL and the weight of WTR was varied. The result of this study was shown in Figure 4.6

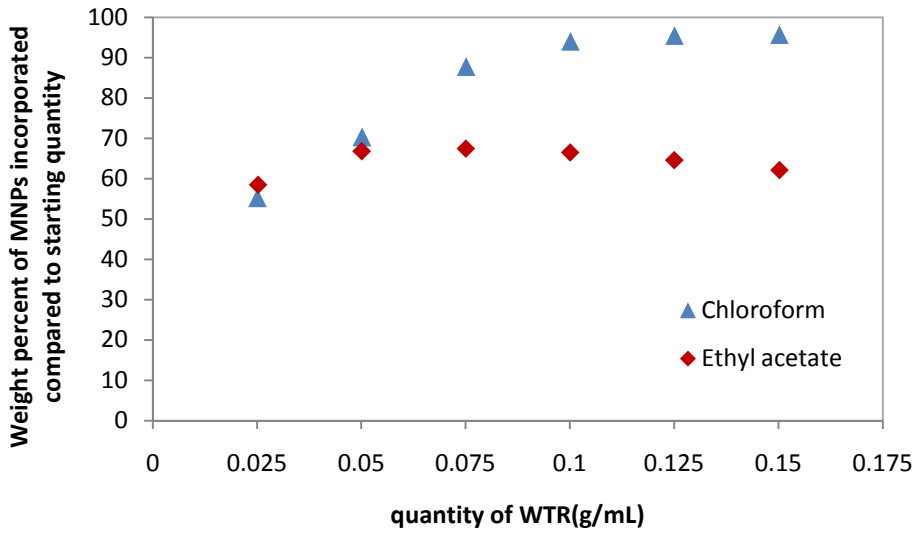

Figure 4.6 Effect of the quantity of WTR to percent removal of MNPs.

This graph shows percent removal of MNPs with different WTR quantities when the same starting concentration of MNPs was used. The result showed that in chloroform the percent removal of MNPs increased according to the quantity of WTR and reached the maximum percent removal of 95 when WTR of 0.1 g/mL was used. The percent removal of MNPs also keep increasing with small percent when WTR of more that followed quantity of WTR. In case of ethyl acetate, the maximum percent removal of MNPs was 70 and the percent removal decreased when WTR of more than 0.075 g/mL was used. From this study, it was another support to use chloroform rather than ethyl acetate due to a lower maximum percent removal was obtained in ethyl acetate system.

4.5 Characterization

The WTR/MNPs composites were characterized by various techniques including FT-IR, XRD, TGA, SEM, and magnetometry. The properties and characteristics of the composites will be discussed in the following sections.

4.5.1 FTIR

FTIR was used to identify the bonding and functional groups existing in the composites. In this research, two samples were characterized, the composites (Figure 4.8) and the MNPs (Figure 4.7) used for comparison.

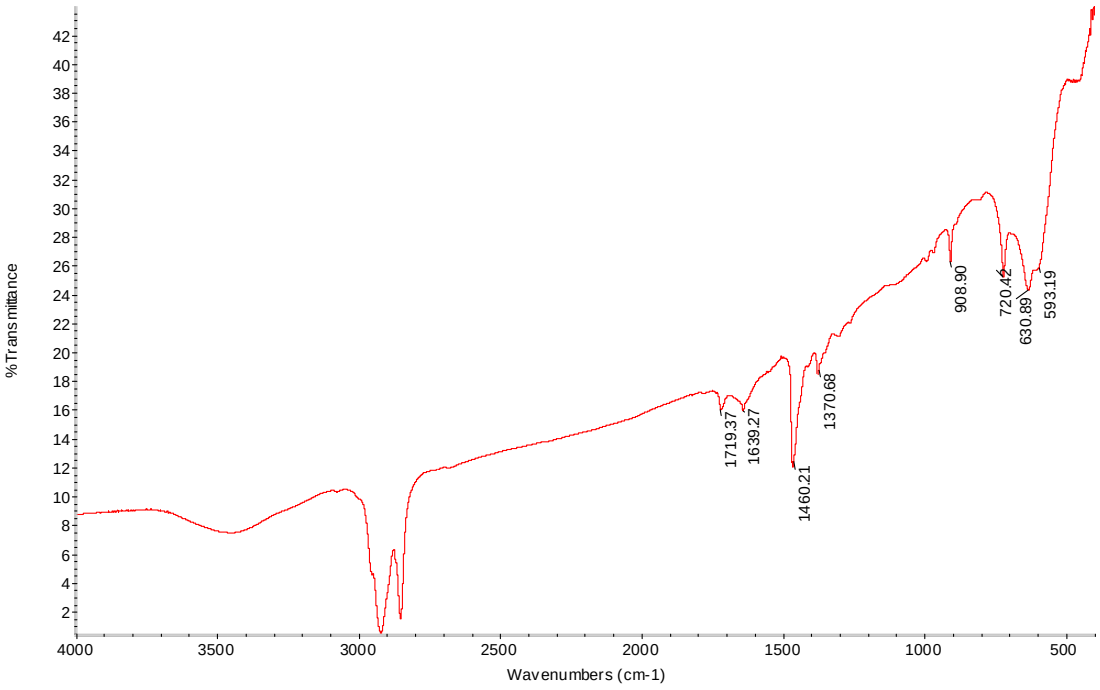

Figure 4.7 FTIR spectrum of magnetic nanoparticles.

From Figure 4.7, the FT-IR transmittance spectrum of MNPs showed the Fe – O bonds at 582 and 640 cm^{-1} that indicated the stretching vibrations of the metal-oxygen absorption band [51]. The characteristic peaks of γ-Fe_2O_3 were shown at 554, 635, 696, and 735 cm^{-1}, and for Fe_3O_4 phase the characteristic peaks is only at 570 cm^{-1} [52] . The FTIR peak at 1706 cm^{-1} represented the stretching vibration of the C=O (carboxyl group) of oleic acid molecule [51]. Moreover, the C=C stretching mode for oleic acid was

located at 1655 cm^{-1} [53]. The dimeric COOH species showed infrared bands at 1712 cm^{-1} [53]. The O–H out of plane bonds ranged from 935.41 to 838.98 cm^{-1} [51]. The symmetric stretching of – CH_3 and – CH_2 – existed at 2873 and 2852 cm^{-1} and asymmetric ones occurred at 2956 and 2923 cm^{-1} [53]. The oleyl group was associated with 2854 and 2922 cm^{-1} [54]. From the FTIR spectrum, we can conclude that the synthesized MNPs were composed of mixing phases of maghemite and magnetite with oleic acid on the surface of the MNPs.

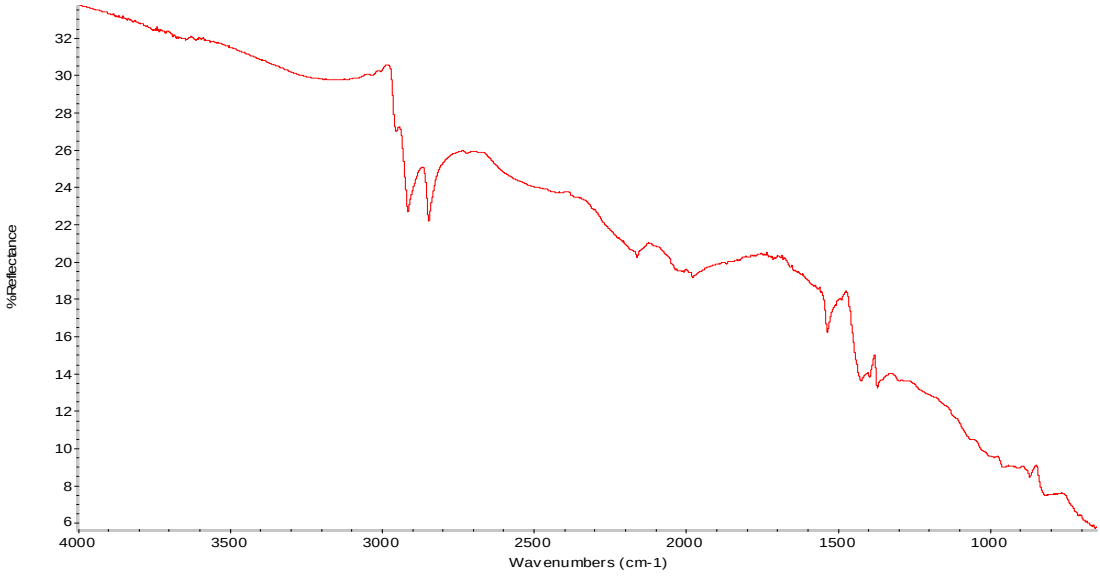

Figure 4.8 FTIR spectrum of the composites prepared using chloroform.

The FT-IR transmittance spectrum of the composites prepared using chloroform is shown in Figure 4.8. The peaks appeared at 3000-2800 cm^{-1} and 1360-1480 cm^{-1} is responsible for the aliphatic C–H stretching vibrations and C–H deformation vibrations, respectively. These peaks indicated the presence of alkanes, which is as expected for rubber. The peaks around 900-675 cm^{-1} region were for C–H out of plane bending peaks indicate the presence of aromatic compounds [55]. Furthermore, the alkyl benzene peaks existed at 2918 and 2875 cm^{-1}, which indicate the presence of aliphatic C–H stretching [55]. The *trans* >C=CH< peaks appeared at 965 cm^{-1}, which is an indication of the aromatic hydrogen [56]. The frequency range of 1021 cm^{-1} peak observed is responsible for the styrene. The NR peaks appeared at 886 cm^{-1} and 1374 cm^{-1} [57].

The a *trans*-butadiene moiety peak was at 964 cm^{-1}, but it cannot distinctly indicate whether this peak was from BR or SBR [57]. The butadiene showed absorption bands at 2914 and 2844 cm^{-1}, which indicated C–H stretching; 1450 cm^{-1} that represented CH_2 in-plane deformation and 1639 cm^{-1} that was responsible for C=C stretching in $CH=CH_2$ groups [58]. From the FTIR spectrum of the composites, we found that the WTR used in this research is composed of NR, SBR, and probably BR. However, the peaks from MNPs cannot be observed in the composite sample due to very low concentration of MNPs in the composites.

4.5.2 XRD pattern of magnetic nanoparticles

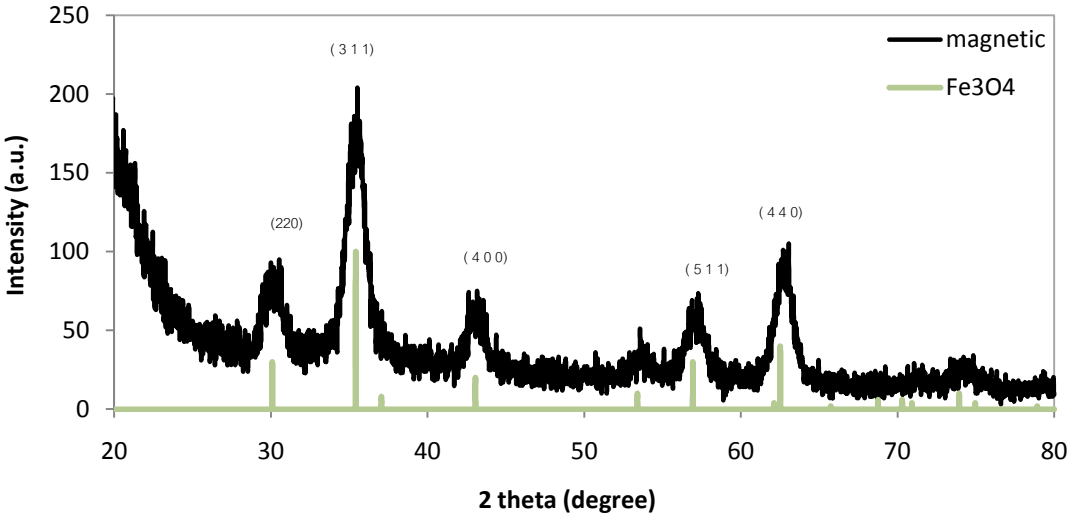

Figure 4.9 The XRD pattern of MNPs.

The XRD pattern of MNPs showed that the phases of MNPs matched with both magnetite (Fe_3O_4) and maghemite (γ-Fe_2O_3) patterns as shown in Figure 4.9. The diffraction peaks of Fe_3O_4 and γ-Fe_2O_3 are so similar that the XRD patterns cannot indicate exactly whether the magnetite or maghemite phases are the dominant phase [59]. However, both of these two phases are ferromagnetic and exhibit spontaneous magnetization as we proposed to obtain.

Moreover, from the XRD pattern of the MNPs, the particle sizes of the MNPs can be calculated. The particle size was calculated using Scherrer equation (4.1) [43].

The reflection peak at (3 1 1) plane was used to calculate the particle size as it is the peak with highest intensity.

$$D = \frac{K\lambda}{(b\cos\theta)} \quad (4.1)$$

where λ is the X-ray wavelength (1.5418 Å), θ is the the angle of the position of the reference peak, *b* is the width at half height of the reference peak, and *K* is a shape factor, which is about 0.9 for magnetite and maghemite.

The estimation of the particle size using the calculation above was approximately 9 nm for the MNPs used. This calculation agrees well with the results obtained from the TEM analysis.

4.5.3 Thermal property of WTR, MNPs, and the composites.

Thermogravimetric analysis (TGA) was used to analyse weight loss by comparison between WTR and composite in relation to changes in temperature. This composite used chloroform as solvent. Thermogravimetric analysis (TGA) was used to analyse the weight loss of the composites in comparison to WTR and MNPs with the relation to changes in temperature. The TGA traces of the composites prepared using various are shown in Figure 4.10. Moreover, differential thermal analysis (DTA) traces of the composites comparing with WTR and MNPs are shown in Figure 4.11.

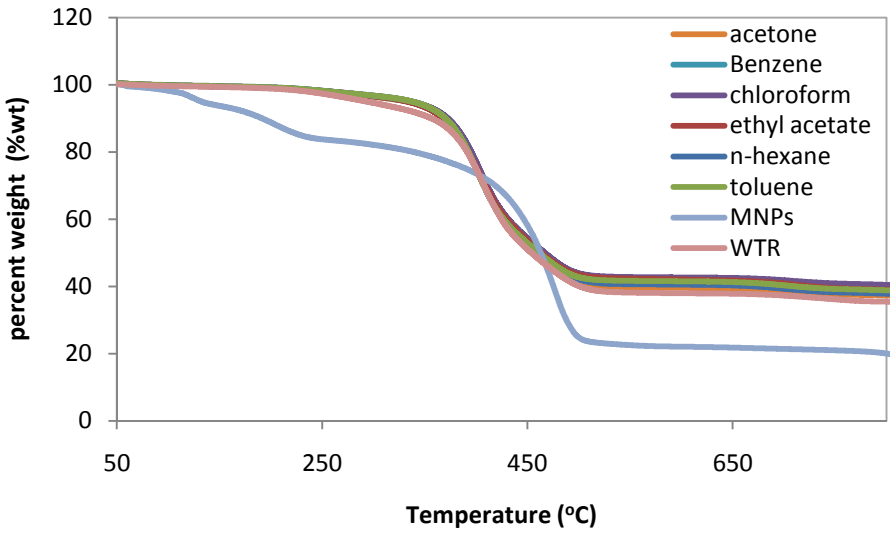

Figure 4.10 TGA traces of the composites compared to WTR and MNPs.

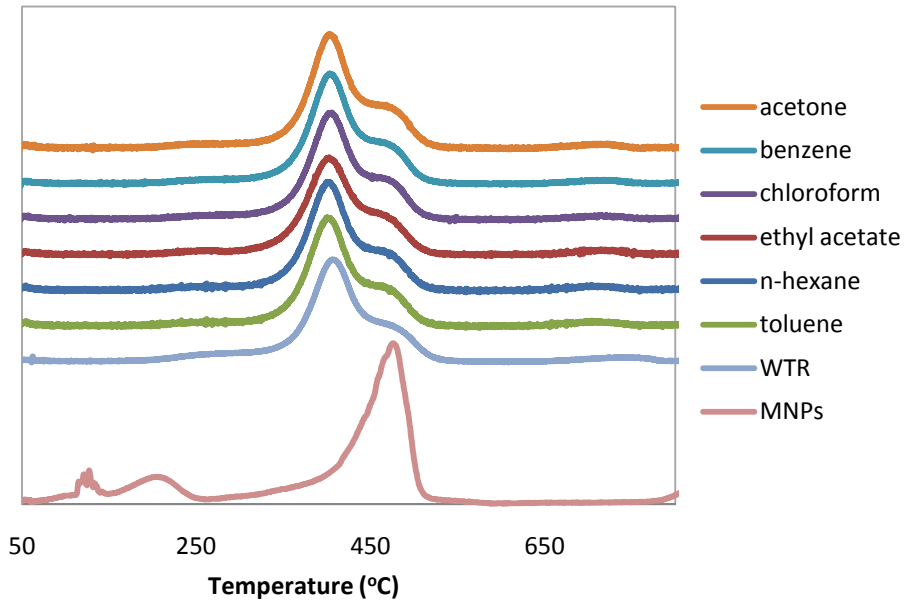

Figure 4.11 DTA traces of the composites compared to WTR and MNPs.

The thermograms of WTR, MNPs and the composites shown in Figure 4.10 were measured by thermogravimetric analysis (TGA). It was found that the initial decomposition temperature of WTR was 300 °C. The weight loss between 200-350 °C was the evaporation or decomposition of extender oil and other organics in WTR [60]. There were two steps in thermal decomposition of WTR and the composites. The first step at 406 °C was most likely the thermo-oxidation of the polymer phase. Based on SBR thermogram, it was observed that the initial thermal decomposition temperature started at ~420°C [61]. The second step at 558 °C was likely the thermo-oxidation of the carbon black [60]. The DTA traces of WTR and the composites also indicated degradation two steps more clearly at the temperature of 406 °C and 475 °C as shown in Figure 4.11.

The weight of residues of all composites left at 700 °C was increasing from acetone, ethyl acetate, toluene, benzene, and chloroform, respectively. The weight of residues were in direct relation with the percent loading of MNPs which was measured using UV-Visible spectrometer as mentioned in Section 4.4.

For the TGA and DTA of the MNPs, the temperature of degradation of MNPs was higher than WTR. The weight loss in the thermogram of MNPs showed that the moisture was eliminated at 120 °C. The thermal desorption and dehydrogenation of oleic acid

were at 200 °C and 400 °C [62]. The pathway of oleate ligand degradation was shown in thermogram that at 200 - 240 °C one oleate ligand dissociated from the MNPs. Carbon dioxide was eliminated from two oleate ligands at ~300 °C [46].

From the comparison of thermograms of WTR and the composites indicated difference of degradation temperature between WTR and composite due to the composites possessing MNPs inside. This result can imply that the composites have MNPs embedded inside the polymer chain of WTR.

4.5.4 SEM Images of composite

The SEM micrograph revealed the morphologies of WTR and the composites. WTR particles showed both rough and smooth surfaces, with irregular shapes as shown in Figure 4.12. The roughness surface can enhance the sorbent efficiency due to better locking-oil capability [49]. The composites synthesized using chloroform as solvent were found to be similar to WTR even though it has MNPs distributed on WTR surfaces.

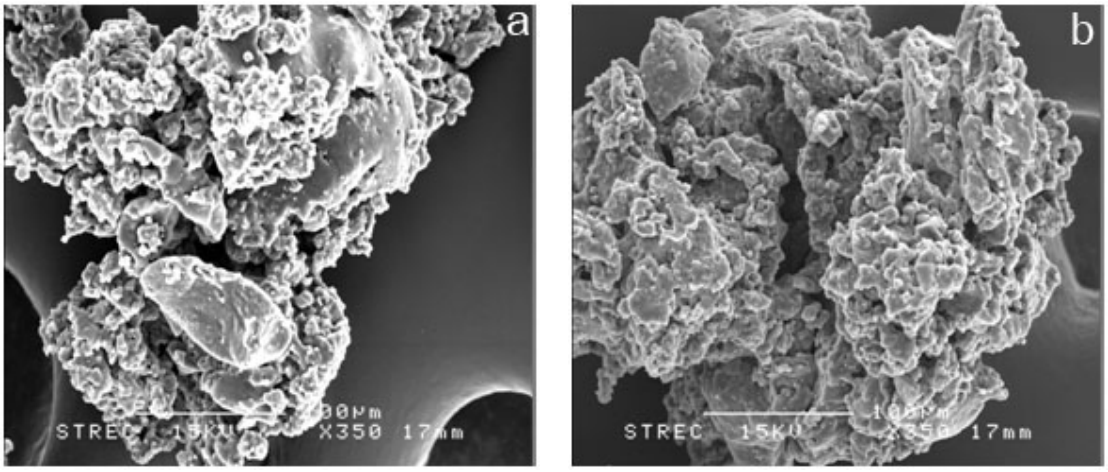

Figure 4.12 The SEM micrographs WTR (a) WTR/MNPs composite, which was synthesized by chloroform (b).

The Energy Dispersive X-Ray Spectrometer (EDX) spectra measured from the same area as in SEM micrograph were an indication that MNPs were on the composites as there were iron signal observed in the composites using chloroform in the synthesis. Quantity of iron on WTR and the composite synthesized using chloroform are shown in Figure 4.13.

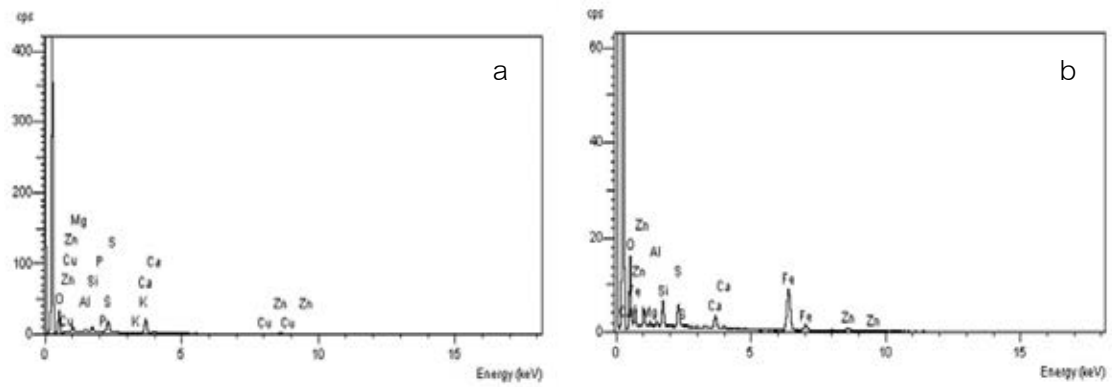

Figure 4.13 EDX spectra on surface of WTR (a) and the composites synthesized using chloroform (b).

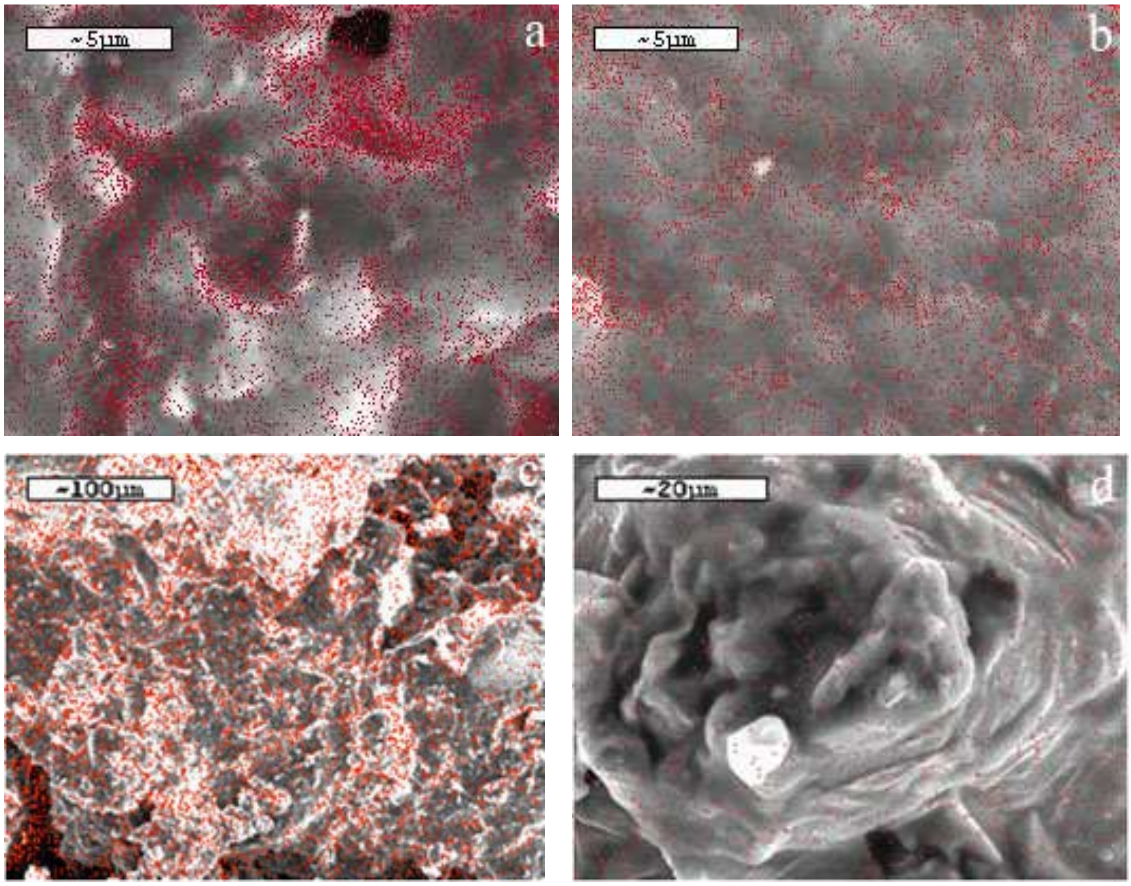

Figure 4.14 The SEM micrographs and EDX elemental mapping of the composites synthesized using ethyl acetate (a) and chloroform (b). The micrographs of the composites synthesized using chloroform with the EDX elemental mapping on surface of composites (c) and inside the composite matrix (d). Red spots indicate the area where iron signal was detected.

Moreover, using elemental mapping mode equipped with SEM and EDX, it was found that the MNPs have distributed in all area of the WTR composites synthesizing using ethyl acetate and chloroform, indicating that the MNPs can embed into WTR matrices. However, when comparing the distribution of the MNPs in the composite synthesized using chloroform, which was shown in Figure 4.14 (b), the MNPs distributed and dispersed better than the composite using ethyl acetate (Figure 4.14 (a)). The reason for the differences in MNPs distribution is likely due to the polarity of each solvent. As the non-polar oleate-coated MNPs can disperse in chloroform better than in ethyl acetate, the MNPs are less agglomerated and dispersed more evenly in chloroform. However, the quantity of MNPs on surface WTR was more than MNPs dispersed more deeply inside WTR matrix as shown in Figure 4.14 (c) and (d).

The combination of desired MNPs in the composites depends on physical and chemical properties of MNPs and polymer. The composites can be obtained in a variety of structures. There are several the formation patterns of MNP-polymer composites as shown in Figure 4.15.

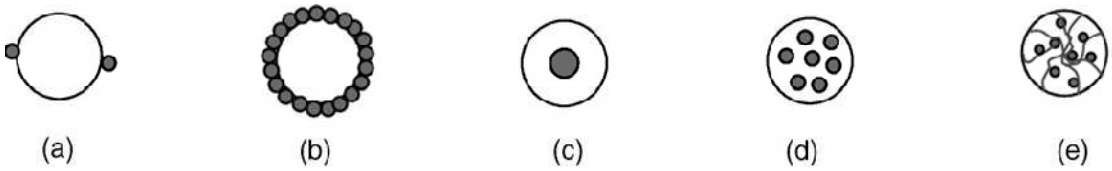

Figure 4.15 The possible structures of MNPs and polymer composite particles.

(a) A few magnetic grains tagged onto the external surface of polymer microspheres.
(b) Magnetic grains coated on the external surface of polymer microspheres.
(c) A single magnetic grain coated by a polymer.
(d) Multiple magnetic grains embedded in a polymer matrix.
(e) Magnetic materials deposited in the internal pores of a polymer matrix.

The SEM images indicated arranging MNPs in WTR following the Patterns a and d in Figure 4.15 because MNPs were observed to distribute on surface of composites in Figure 4.14 (c) and inside the composite matrix in Figure 4.14 (d) as shown MNPs

embedded in the composite matrix. The release of MNPs during and after the use were discussed in Section 4.9.

4.5.5 Magnetization of WTR/MNPs composites

The magnetic properties of the MNPs are of interest for the application as sorbent of the composites. In this research, MNPs are an important part for the disposal of the used sorbents out of water by mean of magnetic separation. The magnetic properties of the WTR and the composites were shown in the forms of the saturation magnetization (Ms), the remanence magnetization (Mr) and the coercivity (Hc). The magnetization for composites was analyzed using a vibrating sample magnetometer (VSM) in order to determine magnetization of MNPs shown in Figure 4.16. The magnetization was measured by applying magnetic fields of -10000 to 10000 G to each sample.

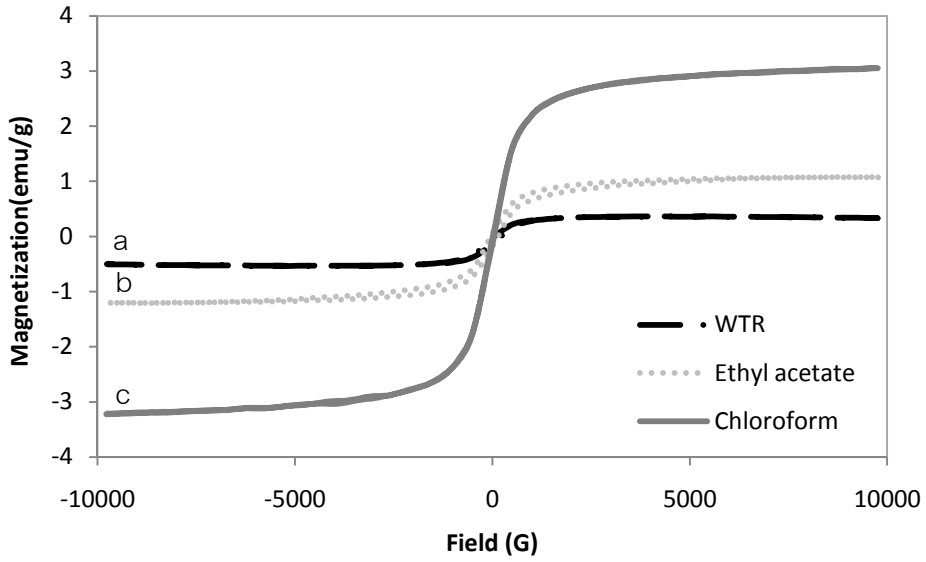

Figure 4.16 Magnetization of (a) WTR, (b) the composites synthesized using ethyl acetate, (c) composites synthesized using chloroform.

The saturation magnetization of the composites synthesized using chloroform was 3.14 emu/g while saturation magnetization of the composite synthesized using ethyl acetate was 1.14 emu/g. The magnetization of the composite synthesized using ethyl acetate was lower than that of the composites synthesized using chloroform

because lower percent MNPs loaded into the WTR matrices. Besides, the coercivity was 14.25 G and 94.36 G for the composite synthesized using chloroform and ethyl acetate, respectively. The coercivity of the hysteresis loops indicate that superparamagnetic behavior is less dominant in the composite from ethyl acetate due to the fact that MNPs in the composite from ethyl acetate were less dispersed and there was a higher degree of aggregation of the MNPs.

Part II Absorption study

4.6 Oil sorption

The result of gasoline absorbency of washed WTR using modified ASTM F726-99 method is shown in Figure 4.17.

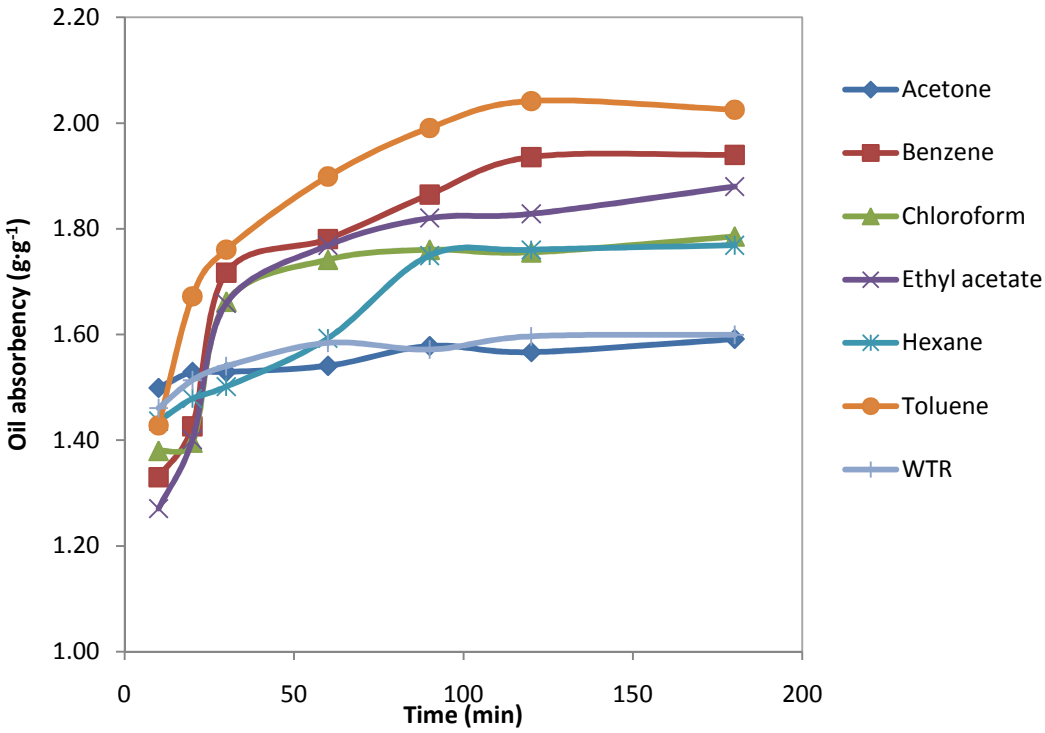

Figure 4.17 Gasoline absorbency of WTR and treated WTR by different washing solvents.

From Figure 4.17, WTR treated by toluene showed the highest oil sorption. The oil absorbency rapidly increased and the maximum sorption capacity was

2.04 ± 0.12 $g \cdot g^{-1}$ at 120 min. The oil absorbency was invariable above 120 min. Furthermore, for treated WTR that was washed with others solvents, the oil absorbencies were 1.94±0.28 $g \cdot g^{-1}$, 1.88 ±0.11 $g \cdot g^{-1}$, 1.79±0.03 $g \cdot g^{-1}$, 1.77±0.19 $g \cdot g^{-1}$, 1.59±0.09 $g \cdot g^{-1}$ when using benzene, ethyl acetate, chloroform, *n*-hexane and acetone, respectively, as washing solvent. Oil absorbency of chloroform treated WTR was nearby that of hexane. The trend of increasing oil absorbency is in accordance with the properties of solvent. And it depended on their solubility parameter and polarity. Toluene washed out a layer of brownish constituents that were composed with the component like toluene which is non-polar. Therefore, toluene washed part of non-polar and exposed part of polar. Gasoline composes of polar component such as ethanol that was used as oxygenated agent to increase the octane [63]. Some non-polar components of WTR was washed out and The surface of WTR was slightly polar, as a result its surface preferred to adsorb a polar compound. In case of acetone, it could not wash out a layer of brownish constituents because oil absorbency was similar to that of WTR.

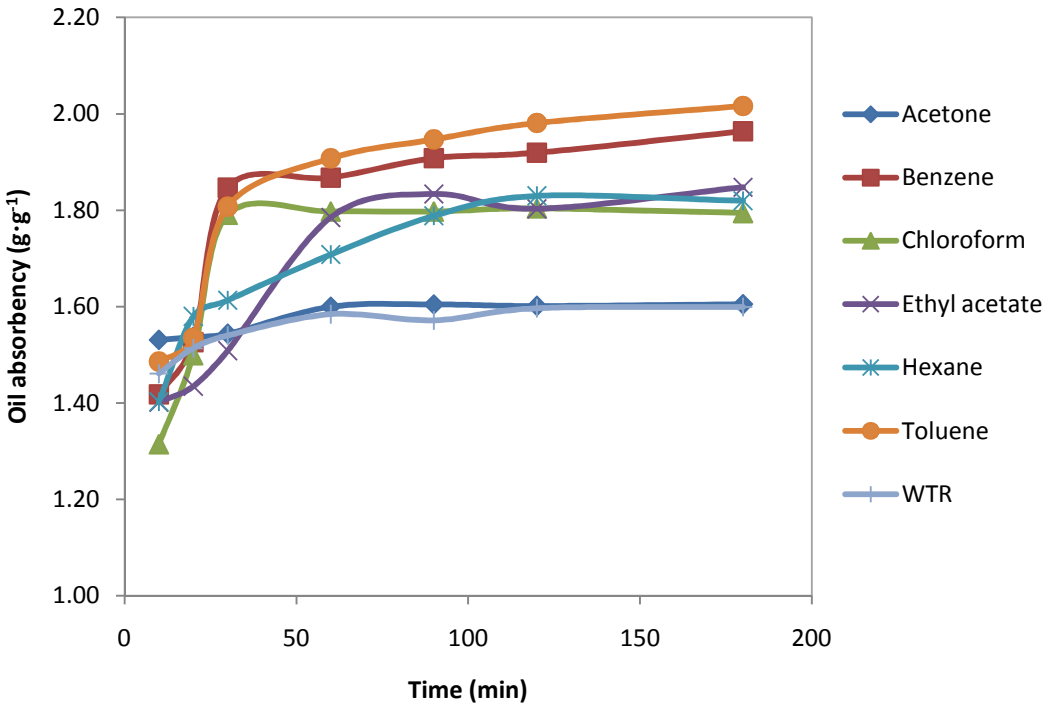

Figure 4.18 Gasoline absorbency of composites having different synthesized solvents.

The oil absorbency of WTR/MNPs composites is shown in Figure 4.18. Toluene treated WTR/MNPs composite showed the highest oil sorption which was similar trend with the results of solvent-treated WTR. The oil absorbency rapidly increased and reached the maximum sorption capacity of 2.01 ± 0.08 $g \cdot g^{-1}$ at 120 min. The oil absorbency was invariable above 120 min. Furthermore, the composites of WTR treated by other solvents showed the oil absorbency of 1.96±0.23 $g \cdot g^{-1}$, 1.84 ±0.18 $g \cdot g^{-1}$, 1.83±0.09 $g \cdot g^{-1}$, 1.80±0.13 $g \cdot g^{-1}$, 1.60±0.08 $g \cdot g^{-1}$ when using benzene, ethyl acetate, *n*-hexane, chloroform and acetone, respectively, as solvent. The oil absorbency of chloroform treated WTR composite was nearby that of hexane. The oil absorbency of solvent washed WTRs and WTR/MNPs composites was quite similar, except for the result of the composite prepared by using ethyl acetate that was lower than ethyl acetate treated WTR probably due to oleic acid (an agent used in MNPs synthesis) attached onto the surface of WTR and made its surface higher hydrophobic. Moreover MNPs aggregated in ethyl acetate but in case of acetone, MNPs had large size of aggregates and showed less percentage of MNPs in the composite.

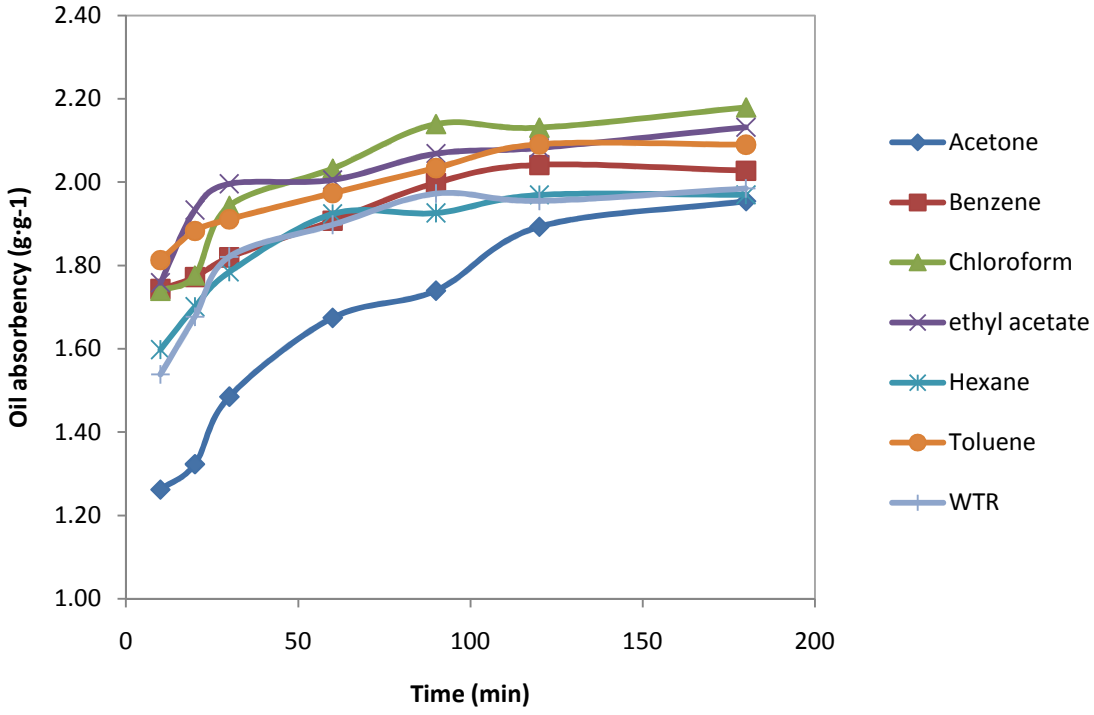

Figure 4.19 Diesel absorbency of WTR and treated WTR by different washing solvents.

The diesel oil absorbency of composites WTR/MNPs is shown in Figure 4.19. Chloroform treated WTR/MNPs showed the highest oil sorption. The oil absorbency rapidly increased and reached the maximum sorption capacity of 2.18 ± 0.01 $g \cdot g^{-1}$ at 100 min. The oil absorbency was invariable above 100 min. Furthermore, the oil absorbencies of other WTR composites were 2.13±0.04 $g \cdot g^{-1}$, 2.09 ±0.10 $g \cdot g^{-1}$, 2.03±0.13 $g \cdot g^{-1}$, 1.97±0.10 $g \cdot g^{-1}$, 1.95±0.05 $g \cdot g^{-1}$ for WTR treated by ethyl acetate, toluene, benzene, *n*-hexane, and acetone, respectively. The results indicated that the oil absorbency depended on the solvent using for cleaning WTR because of different properties of solvent such as solubility parameter and polarity. When washing the WTR by chloroform, the brownish substance was observed on the inner wall of the container. After inspection by IR spectroscopy (data not shown), this non-polar brownish constituent composed of zinc stearate and other unidentified rubber-like compounds. As chloroform is more polar than other solvent such as toluene and benzene, some polar compounds could be washed out from WTR, hence the surface became more hydrophobic. As diesel is hydrophobic, it could be highly absorbed by WTR, as a result of high oil absorbency.

Therefore, chloroform was appropriated solvent to wash WTR for diesel sorbent. Ethyl acetate was nearly polar with chloroform hence it could wash some polar components. Acetone was highly polar than the others which could not wash out a layer of brownish constituents and part of few polar affecting oil absorbency.

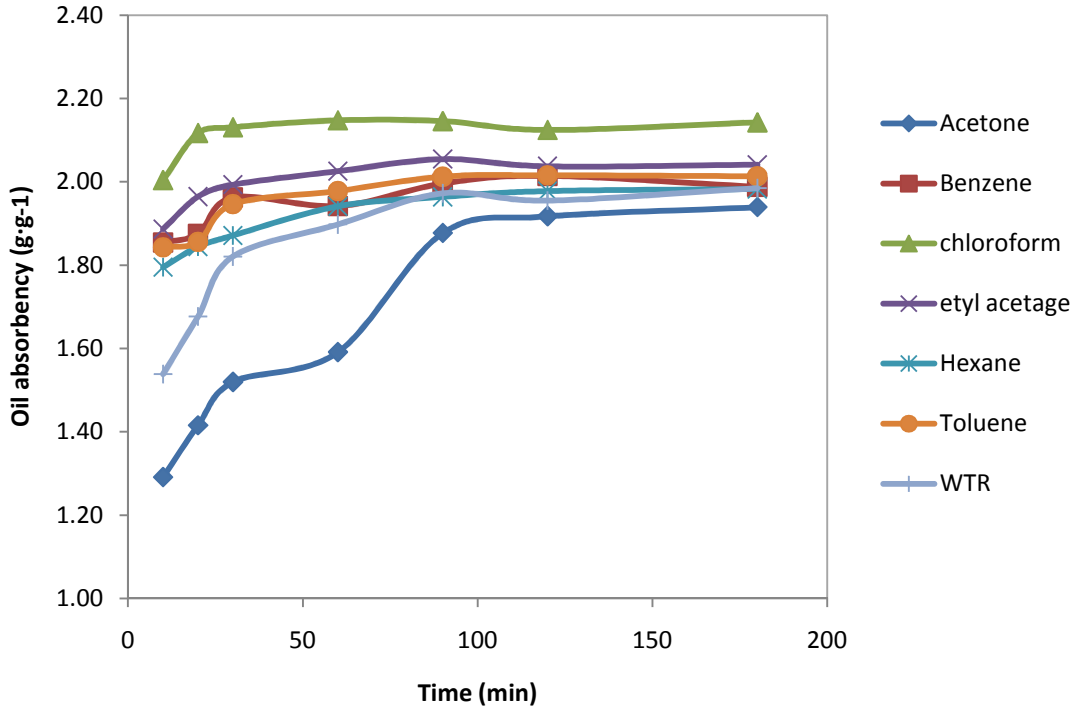

Figure 4.20 Diesel absorbency of composites having different synthesized solvents.

The diesel oil absorbency of washed WTR is shown in Figure 4.20. WTR/MNPs composite using chloroform as preparation solvent showed the highest oil sorption, the same behavior as that presented above for gasoline sorption. The oil absorbency rapidly increased and attained the maximum sorption capacity of 2.14 ± 0.02 $g \cdot g^{-1}$ at 20 min. The oil absorbency was invariable above 20 min. Furthermore, the oil absorbencies of other WTR/MNPs composites were 2.04±0.04 $g \cdot g^{-1}$, 2.01 ±0.21 $g \cdot g^{-1}$, 1.98±0.07 $g \cdot g^{-1}$, 1.98±0.05 $g \cdot g^{-1}$, 1.93±0.28 $g \cdot g^{-1}$ when using ethyl acetate, toluene, benzene, *n*-hexane and acetone, respectively, as preparation solvent. The diesel oil absorbency of treated WTR and composite were similar trend when compared Figure 4.19 and Figure 4.20.

Figures 4.17-4.20 show the increase of oil absorbencies. The slopes indicate the rate of absorption. The rate of oil absorption was fast at the first periods (high slopes), afterwards the slopes declined, indicating that the oil absorption rate became slower. This could be described by a general kinetics of absorption that was controlled

by diffusion. Upon a time, the rate of diffusion decreases when the concentration gradient decreases. In addition, for a long term of immersion, the degradation of polymer network could be occurred [64]. causing by the reaction of solvent, heat, light, and oxygen, hence the absorbency or capacity of absorption could be reduced.

4.7 Synthetic sample

The result is shown in Figure 4.21.

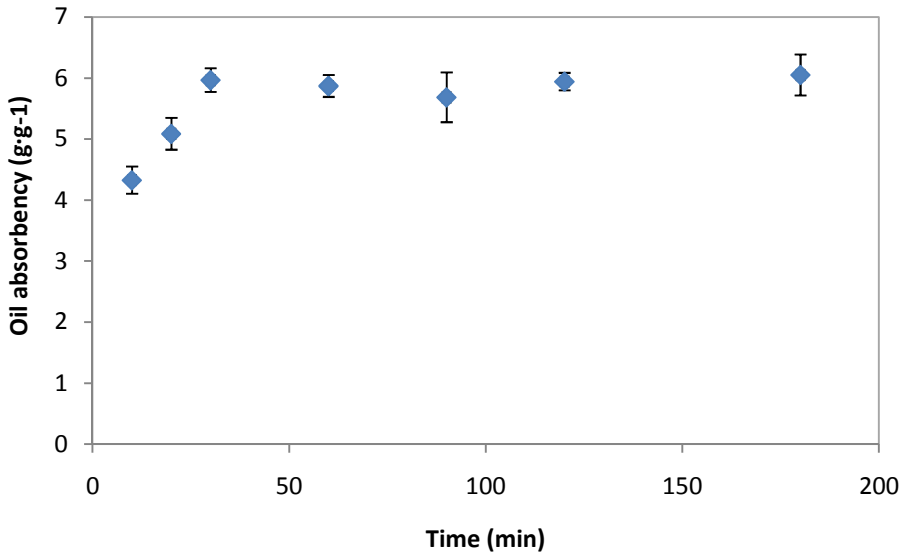

Figure 4.21 Oil absorbency of chloroform synthesized composite for crude oil on water.

The oil absorbency rapidly increased and the maximum sorption capacity was 5.97 ± 0.20 $g \cdot g^{-1}$ at 30 min and it was invariable above 30 min. Composite could be removed from the water surface by means of a permanent magnet that is shown in Figure 4.22.

Figure 4.22 Composite is removed by permanent magnet.

Moreover, the result of crude oil with higher density (ρ=0.937 g/mL) showed high sorption amount, while the gasoline (ρ=0.734 g/mL) showed lower sorption capacity that is shown in Figure 4.23. Therefore, the sorption capacity of sorbent materials depended on the influence of the density of the petroleum products that has been investigated in similar studies. As crude oil is heavier than gasoline and diesel or crude oil has higher average molecular weight than the later, Van Der Walls force depending on molecular weight of absorbate that drives physisorption onto WTR is larger, resulting in higher oil absorbency.

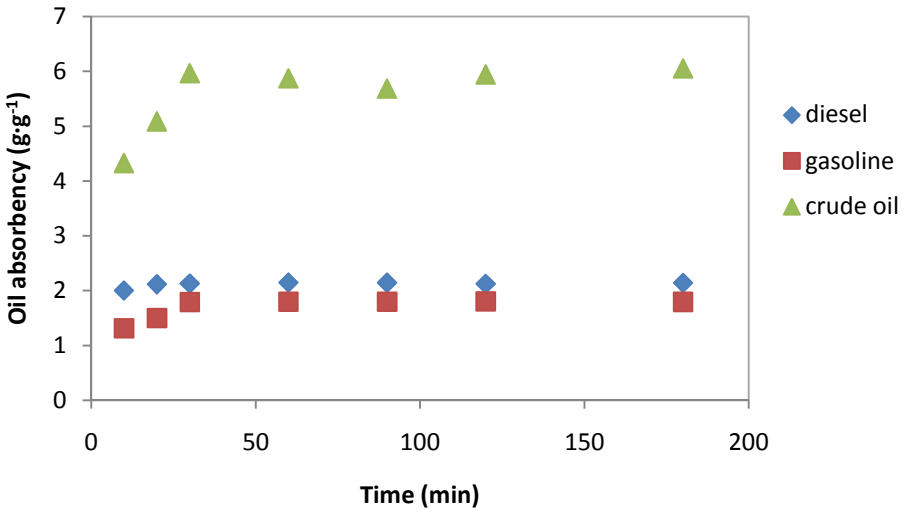

Figure 4.23 Oil absorbency of WTR/MNPs composite using chloroform as preparation solvent.

4.8 Composite sorbent reusability

The reusability of composite was evaluated. WTR/MNPs composite using chloroform as preparation solvent is used for sorbent reusability in diesel.

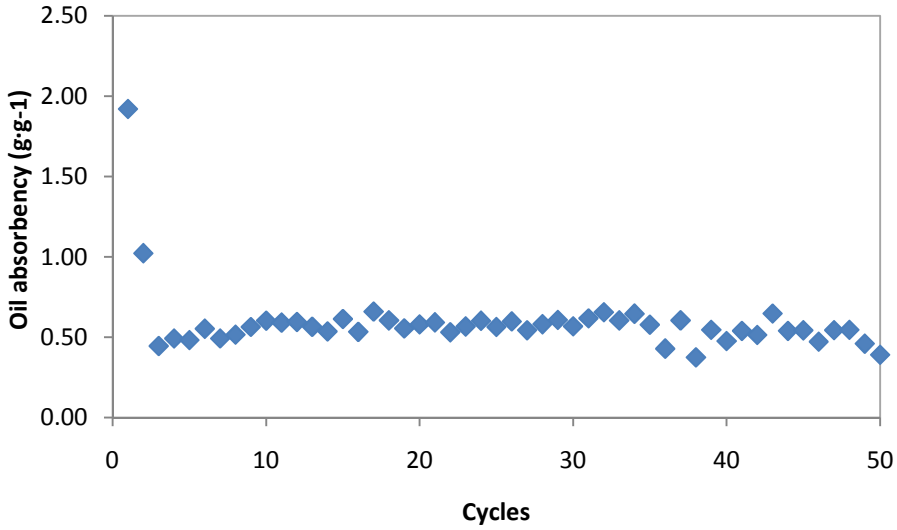

Figure 4.24 Reusability test of composite synthesized by chloroform for diesel absorption.

The reusability result of the composite is shown in Figure 4.24. The reusability test demonstrated the sorption capacity for the first sorption step to be the highest. Over the third cycle, the sorption capacity was invariable. Moreover, the result indicated that the composite can be reused more than 50 times because WTR was an elastic characteristic material and durable. The physical appearance and sorption capacity of the composite did not change, which was around 0.53 ± 0.07 $g \cdot g^{-1}$. This suggesting that the absorption process occurred in the initial times of oil removal, subsequently followed by physical adsorption process. After several cycles of oil removal, the MNPs slightly diffused out from the composite, however the composite could still be removed from the system by using magnetic force.

4.9 Stability of incorporated magnetic nanoparticles in the composites

The stability of sorbent was an important property of the composites to study because MNPs may be released from the composites during their uses. In this research,

we studied the effects from types of oil sorbates and solvents used in the synthesis of composites to the release of MNPs from the composites. The weights of MNPs left in the composites were determined using ICP-OES. In this study, after the composites were used as sorbents, 0.1 g of the separated composites were soaked in 6 mL of concentrated hydrochloric acid and 4 mL of concentrated nitric acid for 24 hr and the mixture was heated until the composites degraded. For the weight of released MNPs, 20 mL of sorbates (diesel and gasoline) were digested using the same procedure. The ICP-OES results are show in Figure 4.25.

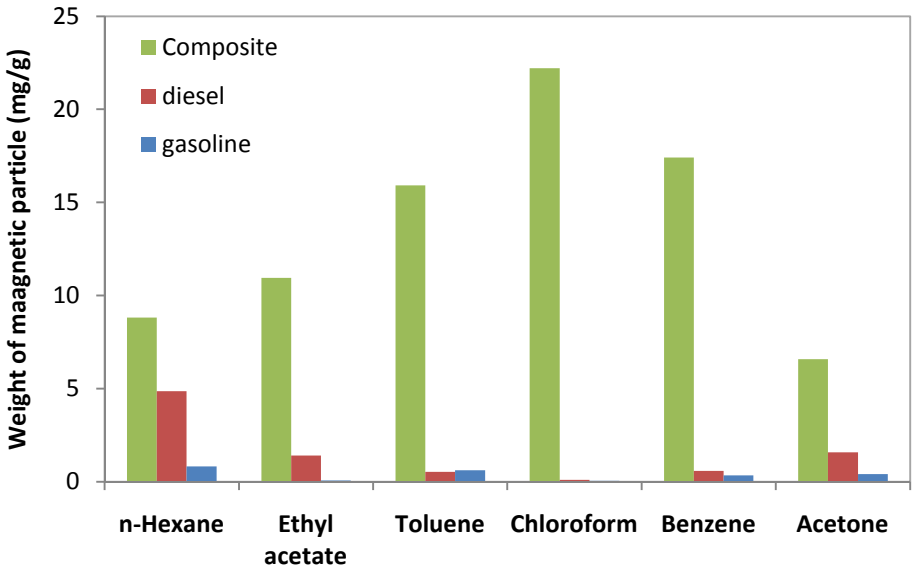

Figure 4.25 Weight of MNPs in the composites (green), and in diesel (red) and gasoline (blue) after the composites were used as sorbents.

The result in the Figure 4.25 showed that the MNPs in the composites determined using ICP-OES were corresponding to the weight of MNPs using UV-Visible spectrometer. This result can confirm that the measurements of weight percent of MNPs in the composites were consistent. Moreover, Figure 4.25 shows the quantity of MNPs left in the composites after their uses. Comparison of each solvent used in the syntheses revealed that chloroform yielded the composites with the most stability toward the release of MNPs as the quantity MNPs in the composites was 22.2 mg/g. In contrast, stability of the composites synthesized in acetone is the lowest as the quantity of MNPs

left in the composites was only 6.6 mg/g. In other solvents, it was found that the stabilities of MNPs in composites were decreasing from the ones synthesized in benzene, toluene, ethyl acetate and *n*-hexane, respectively. The result from this study demonstrates types of solvent affect stability of embedding MNPs in the composites following the same trend as swelling and solubility parameters of the solvents.

MNPs content in diesel and gasoline indicated quantity MNPs released during the soaking of the composites in oil for 30 min. The results revealed that the weight loss of MNPs from the composites synthesized using chloroform was 0.024 mg/g, the lowest among the solvents studied. The reason for the great stability when chloroform is used because WTR can swell greatly in chloroform and MNPs can penetrate deeply into WTR matrix. In contrast, the weight loss of MNPs from the composites synthesized using *n*-hexane was 1.214 mg/g, showing that *n*-hexane is not a suitable solvent for the synthesis of composites. The releases of MNPs in high quantity are likely due to the fact that WTR swelled less in *n*-hexane, resulting in a few MNPs can be embedded deeply into WTR, and the main portion of MNPs was the MNPs deposited on WTR surface. When the composites synthesized using *n*-hexane was soaked in oil, MNPs were released more easily than the composites synthesized using chloroform.

4.10 Separation of the composites from water/oil mixture by a permanent magnet

In order to demonstrate the elimination of diesel on water's surface, the composites synthesized using chloroform were used as sorbent. It was observed that the composites were bounyacy and absorb the diesel oil on the surface of the water/oil mixture. The composite was agglomerated when an external magnetic field was being applied. The demonstration of magnetic separation was shown in Figure 4.26, where the composites were separated out from water by an external magnetic field.

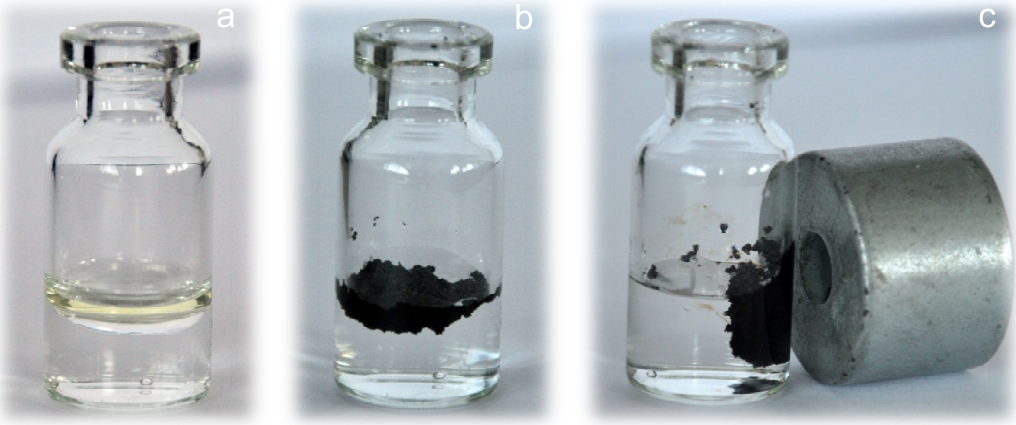

Figure 4.26 Water/oil mixture (a) was used to demonstrate the process of oil sorption (b) followed by magnetic separation of the composites by a permanent magnet (c).

4.11 Magnetic force toward MNPs and the composites [65].

The distance between MNPs and magnet affects the magnetic force. The relationship of distance and the magnetic force generated by a magnetic field was calculated by

$$F = VM\frac{dB}{dx};$$

where F is the magnetic force, V is the volume of the magnetic particle, and M is the magnetization of the magnetic particle and B is the magnetic induction which is the magnetic flux along the axial of a ring magnet that has the analytical form of

$$B = \frac{Br}{2}\left\{\left[\left(\frac{L+x}{\sqrt{R^2+(L+x)^2}}\right)-\left(\frac{L+x}{\sqrt{r^2+(L+x)^2}}\right)\right] - \left[\left(\frac{x}{\sqrt{R^2+x^2}}\right)-\left(\frac{x}{\sqrt{r^2+x^2}}\right)\right]\right\};$$

where Br is the residual induction (Br = 3500 Gauss for NeFeB, magnet used in this experiment), L is the thickness of the magnet, x is the distance between of magnetic particle and the surface of magnet, r is the inner radius of the ring, and R is the outer radius of the ring.

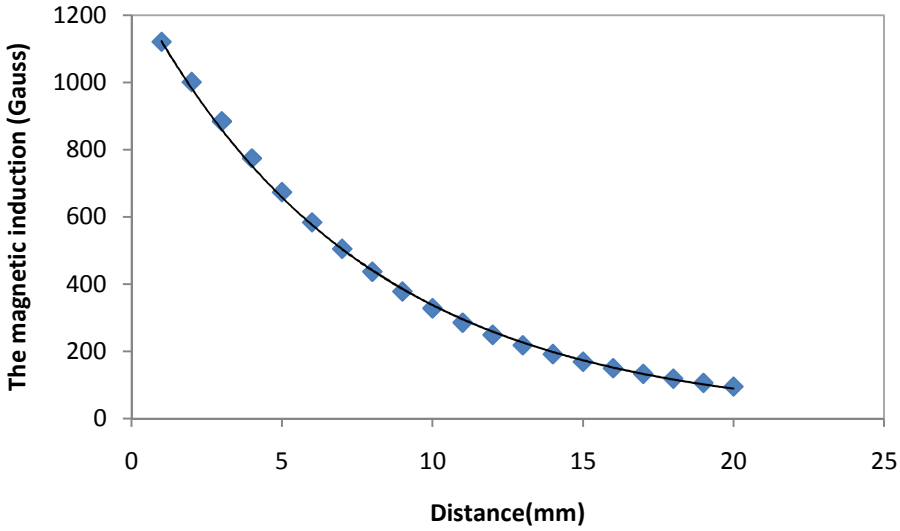

Figure 4.27 The magnetic induction from a NeFeB magnet with the changes in the distance between a magnet and the magnetic particles.

The calculated magnetic flux gradients are presented in Figure 4.27. The maximum force generated by the magnet on a single magnetic particle is about 7.39 pN at the distance of 1 mm. From these calculations, in the real uses, the composites should be as close as possible to the magnet in order to obtain the maximum forces for magnetic separation.

CHAPTER V
CONCLUSION AND SUGGESTION

5.1 Conclusion

Waste tyre rubber-magnetic nanoparticle (WTR/MNPs) composite was synthesized by MNPs solution and WTR. The percentage of MNPs in composite depends on types of solvent, synthesis time, concentration of MNPs, quantity of WTR. The used solvents were acetone, benzene, chloroform, ethyl acetate, *n*-hexane and toluene. The result indicated that chloroform was a suitable solvent. The highest percentage of MNPs in composite is 28.10 % weight at the concentration range of 0.04 - 0.06 g/mL of chloroform. These composites were characterized by Fourier transforms infrared spectrometer (FT-IR), thermogravimetric analyzer (TGA), inductively coupled plasma-optical emission spectrometer (ICP-OES) and scanning electron microscope equipped with energy dispersive X-rays fluorescence spectrometer (SEM-EDX). The result of characterization confirmed that the preparation of MNPs embedded on WTR.

In this research, WTR/MNPs composite could be applied for the sorbent for eliminating oil spill. The sorption capacity test showed that the composites could eliminated oil spill at 25 ^{o}C. The highest sorption capacity of gasoline was achieved using toluene synthesized composite. In case of diesel, the highest sorption capacity was accomplished using chloroform synthesized composite. Furthermore, the removal of crude oil on water surface was studied. The result showed that it can be eliminated by composite. The reusability of the composite was also evaluated. It suggested that the composite could be reused several times over 50 cycles.

5.2 Suggestion

- The further studies should be focused on reclaiming WTR for the high sorption capacity and to improve the percentage of embedded MNPs.

- Other parameter affecting the percentage of embedded MNPs in the composite should be studies such as temperature, pressure, and particle size of WTR.

- The sorption capacity should be studied on more various types of oil such as vegetable oil.

REFERENCES

[1] Jim Group Of Companies. [Online]. 2012. Available from: http://www.abbsrytire.com/tirepiccc333.gif [2012,June 19]

[2] J.E. Mark, B. Erman, F.R. Eirich, (Eds.), The Science and Technology of Rubber, Elsevier Academic Press, UK, 2005.

[3] T. McQuade. [Online]. 2012. Available from: http://www.ehow.com/info_8176244_chemical-properties-tires.html#ixzz22jw4NVWN [2012,June 5]

[4] P.R. Vijayasarathy, Engineering Chemistry, 2nd ed. New Delhi: PHI Learning Private Limited, 2011.

[5] The Agency for Toxic Substances and Disease Registry. [Online]. 1994. Available from: http://www.epa.gov/chemfact/f_trimet.txt [2012,September 2]

[6] Tampereen Teknillinen Yliopisto Tampere University of Technology. [Online]. 2010. Available from: https://www.tut.fi/ms/muo/tyreschool/moduulit/moduuli_4/hypertext_2/2/2_4.html [2011,November 23]

[7] G. Lia, G. Garrick, J. Eggers, C. Abadie, M.A. Stubblefield, S.-S. Pang. Waste tire fiber modified concrete. Composites: Part B 35 (2004): 305-312.

[8] B.V. Kök, H. Çolak. Laboratory comparison of the crumb-rubber and SBS modified bitumen and hot mix asphalt. Construction and Building Materials 25 (2011): 3204-3212.

[9] B. Ellis, M.T. Balba, P. Theile. Bioremediation of oil contaminated land. Environmental Technology 11 (1990): 443-454.

[10] M. Fingas, Oil Spill Science and Technology. USA: Elsevier, 2011.

[11] DAWG. [Online]. 2012. Available from: http://www.dawginc.com/optimax-i-containment-boom-50-l-x-12-draft-x-19-h.html [2012,August 8]

[12] Miyabi Oil Spill Control. [Online]. 2012. Available from: http://www.altimateenvirocare.com/files/downloads/miyabi/MiyabiSpillControlBro03.pdf [2012,October 7]

[13] M. Nomack. Oil spill control technologies. [Online]. 2010. Available from: http://www.eoearth.org/articles/view/158385/?topic=50366 [2012,October 7]

[14] Mavi Deniz enviromental protection services corporation. [Online]. 2010. Available from: http://www.mavideniz.com.tr/product/Sorbents/Sorbents.html [2012,October 15]

[15] A.F.M. Barton, Handbook of Solubility Parameters and Other Cohesion Parameters. Florida: CRC press, 1983.

[16] J. Brydson, Plastics Materials, 7th ed. Oxford: Butterworth-Heinemann, 1999.

[17] D.W.v. Krevelen, K.t. Nijenhuis, Properties of Polymers, 4th ed. Oxford: Elsevier, 2009.

[18] C.M. Hansen, Hansen Solubility Parameters. New York: CRC Press, 2007.

[19] L.R.G. Treloar, The Physics of Rubber Elasticity, 3rd ed. Oxford: Clarendon Press, 1975.

[20] G. Rossi, K.A. Mazich. Macroscopic description of the kinetics of swelling for a cross-linked elastomer or a gel. Physicl Review E 48 (1993): 1182-1191.

[21] L. Ballice. Solvent swelling studies of Goynuk (Kerogen Type-I) and Beypazarı oil shales (Kerogen Type-II). Fuel 82 (2003): 1317-1321.

[22] W.F. Smith, J. Hashemi, Foundations of Materials Science and Engineering. Bangkok: Mc graw hill education, 2008.

[23] M. Schaechter, Encyclopedia of Microbiology, 3rd ed. Oxford: Academic Press, 2009.

[24] W.C. Elmore. Ferromagnetic colloid for studying magnetic structures. Physical Review 54 (1938): 309-310.

[25] Q. Yuan, R.A. Williams. Large scale manufacture of magnetic polymer particles using membranes and microfluidic devices. China Particuology 5 (2007): 26-42.

[26] D. Tarn, C.E. Ashley, M. Xue, E. C.Carnes, J.I. Zink, C.J. Brinker. Mesoporous silica nanoparticle nanocarriers: biofunctionality and biocompatibility. Accounts of Chemical Research 46 (2013): 792-801.

[27] G. Schinteie, V. Kuncser, P. Palade, F. Dumitrache, R. Alexandrescu, I. Morjan, G. Filoti. Magnetic properties of iron–carbon nanocomposites obtained by laser pyrolysis in specific configurations. Journal of Alloys and Compounds 564 (2013): 27-34.

[28] A. Lu, E.L. Salabas, F. Schuth. Magnetic nanoparticles: synthesis, protection, functionalization, and application. Angewandte Chemie International Edition 46 (2007): 1222-1244.

[29] X. Zhang, H. Wang, C. Yang, D. Du, YueheLin. Preparation, characterization of Fe_3O_4 at TiO_2 magnetic nanoparticles and their application for immunoassay of biomarker of exposure to organophosphorus pesticides. Biosensors and Bioelectronics 41 (2013): 669-674.

[30] M. Mahmoudi, S. Sant, B. Wang, S. Laurent, T. Sen. Superparamagnetic iron oxide nanoparticles (SPIONs): Development, surface modification and applications in chemotherapy. Advanced Drug Delivery Reviews 63 (2011): 24-46.

[31] A. Figuerola, R.D. Corato, L. Manna, T. Pellegrino. Review from iron oxide nanoparticles towards advanced iron-based inorganic materials designed for biomedical applications. Pharmacological Research 62 (2010): 126-143.

[32] R.M. Cornell, U. Schwertmann, The Iron Oxides Structure, Properties, Reactions, Occurrences and Uses, 2nd ed. Germany: Wiley-vch, 2003.

[33] D. Ceylan, S. Dogu, B. Karacik, S.D. Yankan, O.S. Okay, O. Okay. Evaluation of butyl rubber as sorbent material for the removal of oil and polycyclic aromatic hydrocarbons from seawater. Environmental Science & Technology 43 (2009): 3846-3852.

[34] I. Karakutuk, O. Okay. Macroporous rubber gels as reusable sorbents for the removal of oil from surface waters. Reactive & Functional Polymers 70 (2010): 585-595.

[35] C. Lin, Y.-J. Hong, A.H. Hu. Using a composite material containing waste tire powder and polypropylene fiber cut end to recover spilled oil. Waste Management 30 (2010): 263-267.

[36] C. Lin, C.-L. Huang, C.-C. Shern. Recycling waste tire powder for the recovery of oil spills. Resources, Conservation and Recycling 52 (2008): 1162-1166.

[37] J. Koutsky, G. Clark, D. Klotz. The use of recycle tyre rubber particles for oil spill recovery. Conservation & Recycling 1 (1977): 231-234.

[38] F.A. Aisien, F.K. Hymore, R.O. Ebewele. Comparative absorption of crude oil from fresh and marine water using recycled rubber. Journal of Environmental Engineering 132 (2006): 1078-1081.

[39] B. Wu, M.H. Zhou. Recycling of waste tyre rubber into oil absorbent. Waste Management 29 (2009): 355-359.

[40] D.S. Kerhaw, C. Kulik, S. Pamukcu. Ground rubber: sorption media for ground water containing benzene and o-xylene. Journal of Geotechnical and Geoenvironmental Engineering 123 (1997): 324-334.

[41] J.Y. Kim, J.K. Park, T.B. Edil. Sorption of organic compounds in the aqueous phase onto the tire rubber. Jouurnal of Environmental Engineering 123 (1997): 827-835.

[42] C. Troca-Torrado, M. Alexandre-Franco, C. Fernández-González, M. Alfaro-Domínguez, V. Gómez-Serrano. Development of adsorbents from used tire rubber Their use in the adsorption of organic and inorganic solutes in aqueous solution. Fuel Processing Technology 92 (2011): 206-212.

[43] Y. Sun, M. Ma, Y. Zhang, N. Gu. Synthesis of nanometer-size maghemite particles from magnetite. Colloids and Surfaces A: Physicochemical and Engineering Aspects 245 (2004): 15-19.

[44] M. Song, Y. Zhang, S. Hu, L. Song, J. Dong, Z. Chen, N. Gu. Influence of morphology and surface exchange reaction on magnetic properties of monodisperse magnetite nanoparticles. Colloids and Surfaces A: Physicochem. Eng. Aspects 408 (2012): 114-121.

[45] T. Hyeon, S.S. Lee, J. Park, Y. Chung, H.B. Na. Synthesis of highly crystalline and monodisperse maghemite nanocrystallites without a size-selection process. Journal of the American Chemical Society 123 (2001): 12798-12801.

[46] J. Park, K. An, Y. Hwang, J.-G. Park, H.-J. Noh, J.-Y. Kim, J.-H. Park, N.-M. Hwang, T. Hyeon. Ultra-large-scale syntheses of monodisperse nanocrystals. Nature Materials 3 (2004): 891-895.

[47] M.M. Yallapu, S.F. Othman, E.T. Curtis, B.K. Gupta, M. Jaggi, S.C. Chauhan. Multi-functional magnetic nanoparticles for magnetic resonance imaging and cancer therapy. Biomaterials 32 (2011): 1890-1905.

[48] G. Wypych, Handbook of Solvents ChemTec Publishing, 2001.

[49] J. Wang, Y. Zheng, A. Wang. Effect of kapok fiber treated with various solvents on oil absorbency. Industrial Crops and Products 40 (2012): 178-184.

[50] S.C. George, S. Thomas, K.N. Ninan. Molecular transport of aromatic hydrocarbons through crosslinked styrene-butadiene rubber membranes. Polymer 37 (1996): 5839-5848.

[51] J.A. Lopez, F. González, F.A. Bonilla, G. Zambrano, M.E. Gómez. Synthesis and characterization of Fe3O4 magnetic nanofluid. Revista Latinoamericana de Metalurgia y Materiales 30 (2010): 60-66.

[52] S. Kubuki, K. Shibano, K. Akiyama, Z.n. Homonnay, E. Kuzmann, M. Ristic´, T. Nishida. Effect of the structural change of an iron–iron oxide mixture on the decomposition of trichloroethylene. Journal of Radioanalytical and Nuclear Chemistry 295 (2013): 23-30.

[53] D.H. Lee, R.A.C. Sr. FTIR spectral characterization of thin film coatings of oleic acid on glasses: I. Coatings on glasses from ethyl alcohol. Journal of Materials Science 34 (1999): 139-146.

[54] N. Shukla, C. Liu, P.M. Jones, D. Weller. FTIR study of surfactant bonding to FePt nanoparticles. Journal of Magnetism and Magnetic Materials 266 (2003): 178-184.

[55] B.K. Sharma, Instrumental Methods of Chemical Analysis. Meerut: Krishna Prakashan Media, 2005.

[56] Y. Lei, Z. Tang, L. Zhu, B. Guo. Functional thiol ionic liquids as novel interfacial modifiers in SBR/HNTs composites. Polymer 52 (2011): 1337-1344.

[57] B. Maridass, B.R. Gupta. Recycling of waste tire rubber powder. KGK Kautschuk Gummi Kunststoffe 56 (2003): 232-236.

[58] K. Subramaniam, A. Das, F. Simon, G. Heinrich. Networking of ionic liquid modified CNTs in SSBR. European Polymer Journal 49 (2013): 345-352.

[59] P. Russo, D. Acierno, M. Palomba, G. Carotenuto, R. Rosa, A. Rizzuti, C. Leonelli. Ultrafine magnetite nanopowder: synthesis, characterization, and preliminary use as filler of polymethylmethacrylate nanocomposites. Journal of Nanotechnology 2012 (2012): 1-8.

[60] C.H. Scuracchio, D.A. Waki, M.L.C.P.d. Silva. Thermal analysis of ground tire rubber devulcanized by microwaves. Journal of Thermal Analysis and Calorimetry 87 (2007): 893-897.

[61] M.A. Mohamed. Swelling characteristics and application of gamma-radiation on irradiated SBR-carboxymethylcellulose (CMC) blends. Arabian Journal of Chemistry 5 (2012): 207-211.

[62] V. Pe´rez-Dieste, O.M. Castellini, J.N. Crain, M.A. Eriksson, A. Kirakosian, J.-L. Lin, J.L. McChesney, F.J. Himpsela. Thermal decomposition of surfactant coatings on Co and Ni nanocrystals. Applied Physics Letters 83 (2003): 5053-5055.

[63] J.E. Anderson, D.M. DiCicco, J.M. Ginder, U. Kramer, T.G. Leone, H.E. Raney-Pablo, T.J. Wallington. High octane number ethanol–gasoline blends: Quantifying the potential benefits in the United States. Fuel 97 (2012): 585-594.

[64] E.V. Takeshita, F.A. Piantola, S.M.A.G.U.d. Souza, R.C.R. Nunes, A.n.A.U.d. Souza. Quantification of styrene–butadiene rubber swelling as a function of the toluene content in gasoline: a new method to detect adulterations of fuels. Journal of Applied Polymer Science 127 (2013): 3053-3062.

[65] H. Shang, P.M. Kirkham, T.M. Myers, G.H. Cassell, G.U. Lee. The application of magnetic force differentiation for the measurement of the affinity of peptide libraries. Journal of Magnetism and Magnetic Materials 293 (2005): 382-388.

BIOGRAPHY

Mr.Pheeraphat Niwasanon was born on November 25, 1987 in Ayutthaya. He received the B.Eng. Degree in Petrochemical and Polymeric Materials at Silpakorn University in 2010. Since then, he has been a graduate student studying in the program of Petrochemistry and Polymer Science at Faculty of Science, Chulalongkorn University and finished his study in 2012.

His present address is 80/2 M.1, Maharat, Maharat, Ayutthaya, Thailand 13150, Tel. 083-8835538.